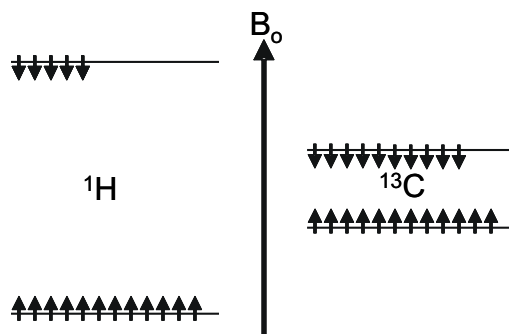
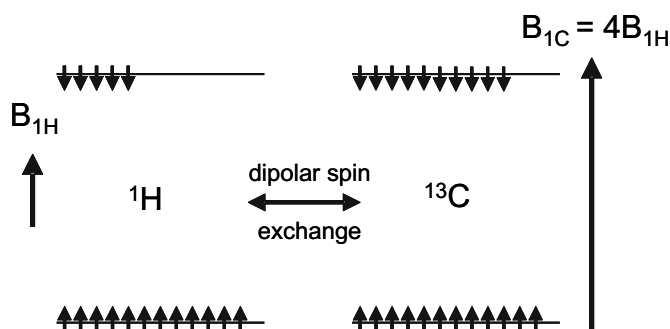


Rotating frame cross relaxation between two sets of spins:

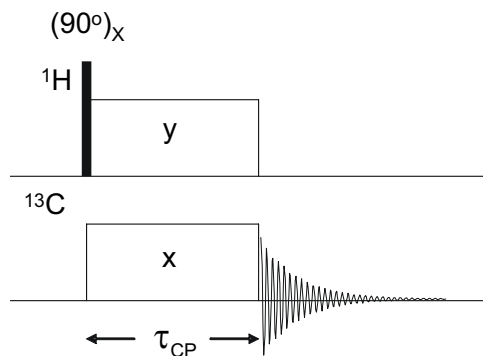
Cross polarization is a technique to transfer magnetization from one set of spins to another. Typically we want to move magnetization from an abundant high γ spin like ^1H and use it to enhance the signal of a rare spin such as ^{13}C . The initial idea of how to do this was cast in the spin temperature concept. The ^1H and ^{13}C nuclei in a sample populate the spin states according to a Boltzmann distribution when placed into a static magnetic field on a time scale determined by T_1 . This population distribution can be used to define the spin's temperature, and for instance if we invert the population with a π pulse the effective temperature becomes negative. In the diagram we schematically indicate the distribution of + and - spin states for ^1H and ^{13}C in the same magnetic field. The excess population in the + state is about 4 times less for the ^{13}C than the ^1H since $\gamma_{\text{H}} \sim 4\gamma_{\text{C}}$.



If we spin lock the magnetizations, the spins experience a much smaller effective magnetic field, at least in the rotating frame, and the spin states will re-equilibrate to a new distribution determined by the “rotating frame” spin temperature, with the effective field being $\frac{\omega_1}{\gamma} = B_1$. Since the two sets of spins are affected by RF fields at different frequencies, we can set the fields to be different, and this makes it possible to set the spin state energy differences to the same value in the rotating frame by adjusting $B_{1\text{H}} = \frac{\gamma_{\text{C}}}{\gamma_{\text{H}}} B_{1\text{C}}$.



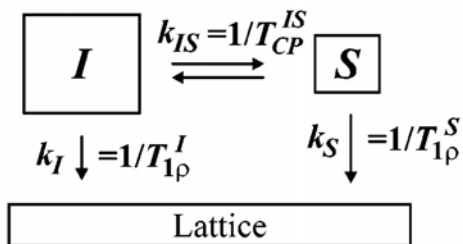
Both sets of spins want to re-equilibrate, and seeing a much smaller B_1 fields the populations will adjust to a much smaller population difference. However, the two sets of spins are usually more strongly coupled to each other than their surroundings, and they tend to equilibrate to a common spin temperature more rapidly by dipole coupling mediated mutual spin flips. If these spin flips are energy conserving the equilibration by this cross relaxation can be much faster than the equilibration with the lattice, the result being a greatly enhanced ^{13}C magnetization. Setting the rotating frame spin state energy splitting the same for both types of spin is known as the Hartmann-Hahn condition.



The typical pulse sequence is diagrammed above. The ^1H magnetization is spin-locked by applying a 90° pulse with phase x , followed by a continuous RF field phase shifted by 90° . This places the ^1H magnetization anti-parallel to this y -phase RF field in the rotating frame. Turning on a ^{13}C RF field with the proper amplitude to satisfy the Hartmann-Hahn condition maximizes the cross-relaxation rate, and a ^{13}C magnetization will grow in a spin locked state along this field. Since the ^1H were prepared in this example anti-parallel to the spin lock field, the ^{13}C magnetization will also grow anti-parallel to the ^{13}C RF field. The resulting ^{13}C signal will have a phase of $-x$ then.

Rate matrix approach

The simplest way to treat a CP transfer is as a cross relaxation process in the rotating frame, analogous to cross relaxation between two sets of spins in the laboratory frame.



The spins can cross relax with each other, or relax back to the lattice. Our treatment will draw on a relaxation matrix formalism used by several authors(1-6). We start following Jeener(2) and consider two types of spins, A and B, numbers of spins n_A and n_B . The usual equations describing the time evolution of the departure of z-magnetization from equilibrium are

$$\frac{d}{dt} \mathbf{m} = -\mathbf{R} \cdot \mathbf{m}$$

where the difference magnetization vector \mathbf{m} is given by

$$\begin{pmatrix} m_A \\ m_B \end{pmatrix} = \begin{pmatrix} M_{zA} - \frac{n_A}{N} M_o \\ M_{zB} - \frac{n_B}{N} M_o \end{pmatrix} = \begin{pmatrix} M_{zA} - M_{oA} \\ M_{zB} - M_{oB} \end{pmatrix}$$

The z-magnetization of each type of spin is denoted M_{zi} and the total z-magnetization of the N spins is M_o . The relaxation matrix \mathbf{R} is written

$$\mathbf{R} = \begin{pmatrix} R_{AA} & R_{AB} \\ R_{BA} & R_{BB} \end{pmatrix}$$

Defining the following quantities following Macura(3)

$$\begin{aligned} \Delta &= \frac{1}{2}(R_{AA} - R_{BB}) = \frac{1}{2}((R_{1A} - R_{BA}) - (R_{1B} - R_{AB})) \\ \sigma &= \frac{1}{2}(R_{AA} + R_{BB}) \\ D &= \sqrt{\Delta^2 + R_{AB}R_{BA}} \\ \eta &= \sqrt{(D + \Delta)^2 + R_{AB}R_{BA}} \end{aligned}$$

it is straightforward to specify a transformation $\mathbf{T}_R^{-1} \cdot \mathbf{R} \cdot \mathbf{T}_R$ that will diagonalize \mathbf{R} :

$$\mathbf{T}_R = \frac{1}{\eta} \begin{pmatrix} D + \Delta & -R_{AB} \\ R_{BA} & D + \Delta \end{pmatrix} \quad \mathbf{T}_R^{-1} = \frac{1}{\eta} \begin{pmatrix} D + \Delta & R_{AB} \\ -R_{BA} & D + \Delta \end{pmatrix}$$

The resulting eigenvalues of \mathbf{R} are then found to be

$$\lambda_{1,2} = \sigma \pm D$$

The general solution to the differential equation for \mathbf{m} is

$$\mathbf{m}(t) = e^{-Rt} (\mathbf{m}(0) - \mathbf{m}(\infty)) + \mathbf{m}(\infty)$$

where the relaxation propagator is easily evaluated using \mathbf{T}_R giving

$$\begin{aligned}
e^{-\mathbf{R}t} &= e^{-\mathbf{T}_R \cdot \mathbf{T}_R^{-1} \cdot \mathbf{R} \cdot \mathbf{T}_R \cdot \mathbf{T}_R^{-1} t} = \mathbf{T}_R \cdot \begin{pmatrix} e^{-\lambda_1 t} & 0 \\ 0 & e^{-\lambda_2 t} \end{pmatrix} \cdot \mathbf{T}_R^{-1} \\
&= e^{-\sigma t} \begin{pmatrix} \cosh(Dt) - \frac{\Delta}{D} \sinh(Dt) & -\frac{R_{AB}}{D} \sinh(Dt) \\ -\frac{R_{BA}}{D} \sinh(Dt) & \cosh(Dt) + \frac{\Delta}{D} \sinh(Dt) \end{pmatrix}
\end{aligned}$$

The magnetization either aligned along z or spin-locked at the end of a cross relaxation period t then has two components

$$\begin{aligned}
M_A(t) &= e^{-\sigma t} \left\{ \left(\cosh(Dt) - \frac{\Delta}{D} \sinh(Dt) \right) (M_A(0) - M_A(\infty)) - \frac{R_{AB}}{D} \sinh(Dt) (M_B(0) - M_B(\infty)) \right\} + M_A(\infty) \\
M_B(t) &= e^{-\sigma t} \left\{ \left(\cosh(Dt) + \frac{\Delta}{D} \sinh(Dt) \right) (M_B(0) - M_B(\infty)) - \frac{R_{BA}}{D} \sinh(Dt) (M_A(0) - M_A(\infty)) \right\} + M_B(\infty)
\end{aligned}$$

Spin-locked cross polarization

In a classic CP experiment between two sets of spin 1/2 nuclei we equate

$$R_{AA} = \frac{1}{T_{1\rho A}} + \frac{1}{T_{AB}} \quad \text{and} \quad R_{BB} = \frac{1}{T_{1\rho B}} + \frac{n_A}{n_B} \frac{1}{T_{AB}}.$$

If the rare spin is A, and B represents the abundant spins, we can write $R_{AB} = -\frac{1}{T_{AB}}$ and $R_{BA} = -\frac{n_A}{n_B} \frac{1}{T_{AB}}$. The equilibrium spin locked

magnetizations $M_A(\infty) = M_B(\infty) = 0$ for CP. In this case, assuming $\frac{n_A}{n_B}$ is very small,

appropriate for the A spins being natural abundance ^{13}C and the B spins being ^1H

$$\Delta = \frac{1}{2}(R_{AA} - R_{BB}) = \frac{1}{2} \left(\left(\frac{1}{T_{1\rho A}} + \frac{1}{T_{AB}} \right) - \left(\frac{1}{T_{1\rho B}} + \frac{n_A}{n_B} \frac{1}{T_{AB}} \right) \right) \approx \frac{1}{2} \left(\frac{1}{T_{1\rho A}} - \frac{1}{T_{1\rho B}} + \frac{1}{T_{AB}} \right)$$

$$\sigma = \frac{1}{2}(R_{AA} + R_{BB}) = \frac{1}{2} \left(\frac{1}{T_{1\rho A}} + \frac{1}{T_{AB}} + \frac{1}{T_{1\rho B}} + \frac{n_A}{n_B} \frac{1}{T_{AB}} \right) \approx \frac{1}{2} \left(\frac{1}{T_{1\rho A}} + \frac{1}{T_{AB}} + \frac{1}{T_{1\rho B}} \right)$$

$$D = \sqrt{\Delta^2 + R_{AB}R_{BA}} \approx \Delta \quad \eta = \sqrt{(D + \Delta)^2 + R_{AB}R_{BA}} \approx D + \Delta$$

$$D + \sigma = \frac{1}{T_{1\rho A}} + \frac{1}{T_{AB}} \quad D - \sigma = -\frac{1}{T_{1\rho B}}$$

The kinetics of the A spin buildup from an initial state of zero then to a CP time of τ is

$$\begin{aligned}
M_A(\tau) &= -M_B(0) e^{-\sigma\tau} \frac{R_{AB}}{D} \sinh(D\tau) = -M_B(0) e^{-\sigma\tau} \frac{R_{AB}}{D} \frac{e^{D\tau} - e^{-D\tau}}{2} \\
&= -M_B(0) \frac{\frac{1}{T_{AB}}}{\frac{1}{T_{1\rho A}} - \frac{1}{T_{1\rho B}} + \frac{1}{T_{AB}}} \left(e^{(D-\sigma)\tau} - e^{-(D+\sigma)\tau} \right) = M_B(0) \frac{1}{1 + \frac{T_{AB}}{T_{1\rho A}} - \frac{T_{AB}}{T_{1\rho B}}} \left(1 - e^{-2D\tau} \right) e^{(D-\sigma)\tau} \\
&= M_B(0) \frac{1}{1 + \frac{T_{AB}}{T_{1\rho A}} - \frac{T_{AB}}{T_{1\rho B}}} \left(1 - e^{-\left(\frac{\tau}{T_{1\rho A}} + \frac{\tau}{T_{1\rho B}} + \frac{\tau}{T_{AB}}\right)} \right) e^{\left(\frac{\tau}{T_{1\rho B}}\right)}
\end{aligned}$$

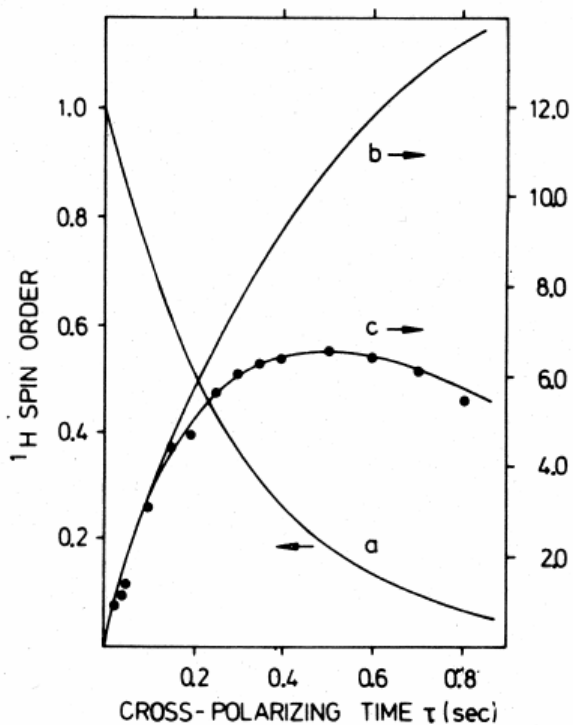
If $T_{AB} \ll T_{1\rho A}, T_{1\rho B}$

$$M_A(\tau) \approx M_B(0) \left(1 - e^{-\frac{\tau}{T_{AB}}} \right) e^{\left(\frac{\tau}{T_{1\rho B}}\right)}$$

For the B spins with these assumptions

$$\begin{aligned}
M_B(t) &= M_B(0) e^{-\sigma t} \left(\cosh(D\tau) + \frac{\Delta}{D} \sinh(D\tau) \right) \approx M_B(0) e^{-\sigma t} \left(\cosh(D\tau) + \sinh(D\tau) \right) \\
&= M_B(0) e^{-\sigma t} \left(\frac{e^{D\tau} + e^{-D\tau}}{2} + \frac{e^{D\tau} - e^{-D\tau}}{2} \right) = M_B(0) e^{-\sigma t} e^{D\tau} = M_B(0) e^{(D-\sigma)\tau} \\
&= M_B(0) e^{-\frac{\tau}{T_{1\rho B}}}
\end{aligned}$$

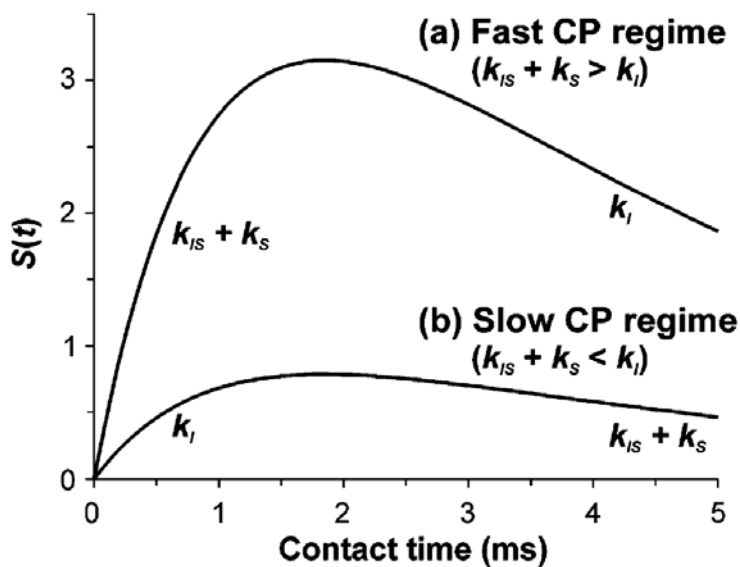
In a typical organic solid $T_{1\rho}$ for the ^1H are 10s of msec, $T_{1\rho}$ for the ^{13}C are 100s of msec, and T_{CH} the order of 100 microseconds. If one observes the abundant spins B the magnetization decays exponentially with time constant $T_{1\rho B}$. The spin locked magnetization for the rare A spin initially grows exponentially towards $M_B(0)$ with a time constant of T_{AB} , while the overall buildup curve is damped by $T_{1\rho B}$ of the B spin bath. An example is shown in the following figure taken from Mehring's text, where the ^{13}C magnetization in adamantane as a function of contact time is fitted to the above equations.



Experimental ^{13}C CP buildup curve fitted to the above description. The decrease in ^1H magnetization is shown in a), buildup of ^{13}C in c). Curve b) is computed assuming no rotating frame relaxation for the ^1H .

Other cases

In some instances T_{AB} is actually longer than the $T_{1\rho}$ of the abundant spin. In this instance it would seem that CP provides no real advantage, and that the rare spin signal that could be built up by CP would be negligible. This turns out not to be the case as shown by Tekely and coworkers. In this limit the time constant for the buildup of magnetization is the abundant spin $T_{1\rho}$, while the decay occurs at the sum of the rare spin $T_{1\rho}$ and the cross relaxation rates.



Mismatch optimized transfers

The thermodynamic treatment assumes strong couplings among both the rare and abundant spins. While this is usually a good assumption for the ^1H in organic solids, it isn't for the ^{13}C at natural abundance. The ^1H - ^1H dipolar interactions broaden the energy level diagram for the protons, but when the RF fields are strong the spin-locked states of the ^{13}C are decoupled and thus narrow. An effective energy level diagram taking into account the ^1H - ^1H interactions is shown below (Wu and Zilm, JMR **93**, 265-278 (1991)).

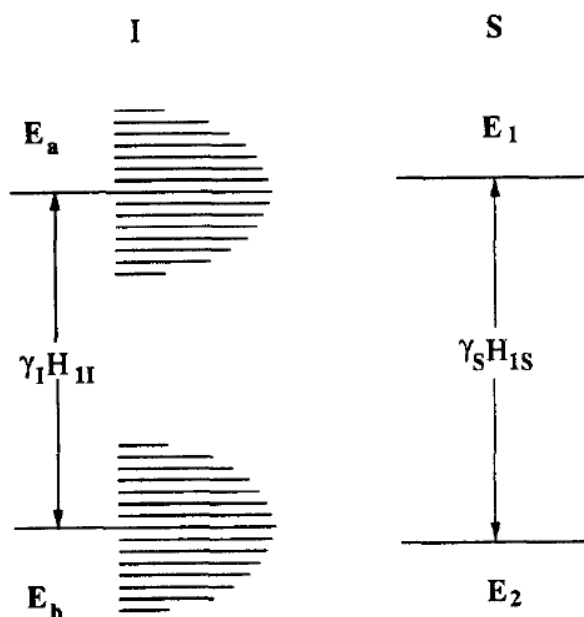


FIG. 1. The energy-level diagram for an SI pair coupling to other I spins. The interaction \mathcal{H}_{II} results in the broadening of the I-spin level, while the broadening of the S-spin level is suppressed by decoupling. The length of the bars in the bands represents the energy-level distribution. This distribution and the width of the bands are determined by the dipolar interaction \mathcal{H}_{II} .

Since the ^1H levels are broad, the Hartmann-Hahn condition is heterogeneous throughout the sample. Different ^{13}C will require different matches to account for local field variations. One consequence of this effect is that a phase shift of the RF fields by 180° , which inverts the spin temperature, will end up satisfying the Hartmann-Hahn condition for a different set of spins. Consider the next figure.

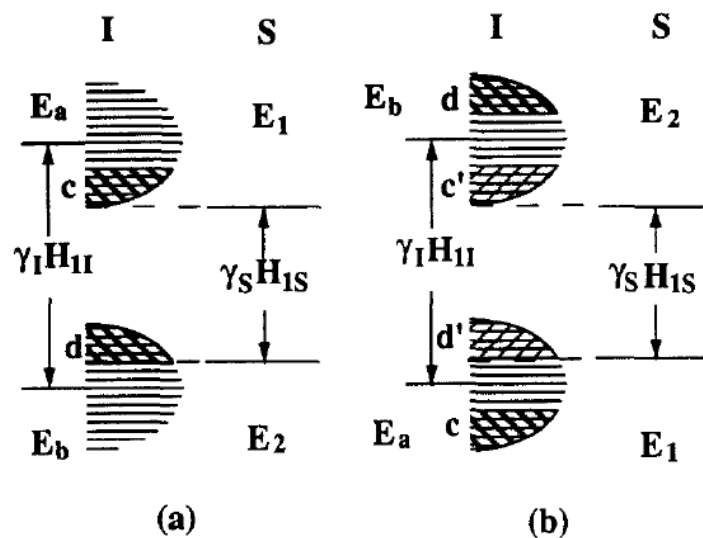


FIG. 2. Under mismatched Hartmann–Hahn conditions, only some of the protons are permitted to take part in the flip-flop with the directly bonded S spin. (a) When $\omega_{IS} < \omega_{I1}$, only those I spins located in shaded areas c and d are in the permitted status. (b) After the phase inversion, the Zeeman energy is inverted, while the dipolar energy is unchanged, so that the two bands exchange their position. In this case, other I spins located in areas c' and d' are in the flip-flop-permitted status, while those in c and d are no longer in the permitted status.

In figure 2a the set of ^1H that will CP to the ^{13}C under a mismatch are indicated by the cross-hatched area of the dipolar broadened energy bands. If the phases of the RF fields are switched by 180° , the spin states are switched, so in effect the populations are also switched. The phase inversion however does not invert the band structure, so as shown in figure 2b a different set of ^1H are brought into the Hartmann-Hahn condition.

One can observe this phenomenon easily in a depolarization experiment. After a CP to the ^{13}C in a sample (static), the ^1H spin lock field is removed and the ^1H magnetization decays. Turning the ^1H RF back on will establish a CP condition that will take polarization away from the ^{13}C to polarize the ^1H , and at the same time depolarize the ^{13}C . The pulse sequences are shown in figure 3.

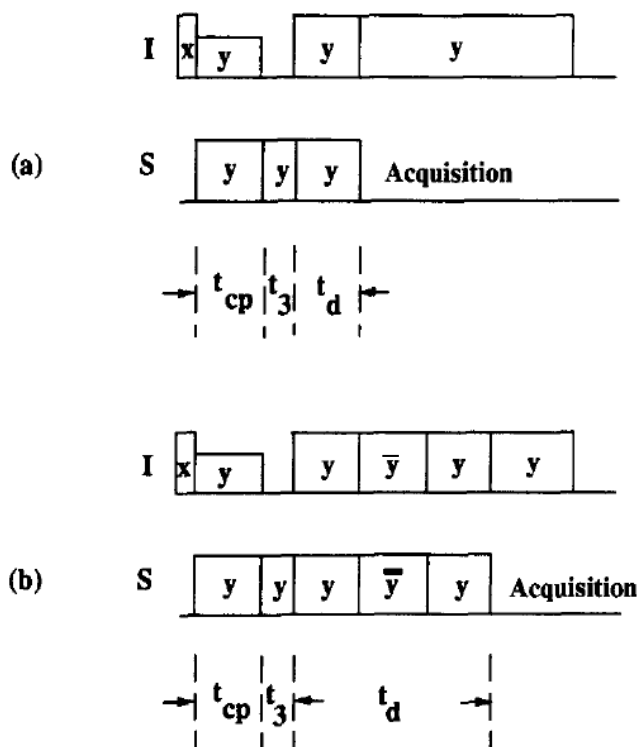


FIG. 3. The pulse sequences utilized. (a) The normal depolarization experiment, where t_{cp} is the cross-polarization time, and t_d is the depolarization time. (b) A modified pulse sequence, where there are synchronous phase reversals of the two irradiation fields during the depolarization.

Using the sequence in figure 3b one can observe depolarization by successive portions of the ^1H bath. Experimental results are shown in figure 7 for a sample of paraformaldehyde ($(\text{CH}_2\text{O})_n$). The ^{13}C signal (at $t = 0$ normalized to 100%) quickly depolarizes, and slowly decays until the simultaneous phase shift at 300 μsec . This brings in a second groups of ^1H s in to depolarize the ^{13}C . At 600 μsec another simultaneous phase shift occurs. The depolarization is much less, since these are the same ^1H s used in the first depolarization interval. The reason a small amount of depolarization is possible in this third interval is that the first group of protons partially re-equilibrated with the rest of the ^1H bath by ^1H - ^1H spin diffusion during the second depolarization time.

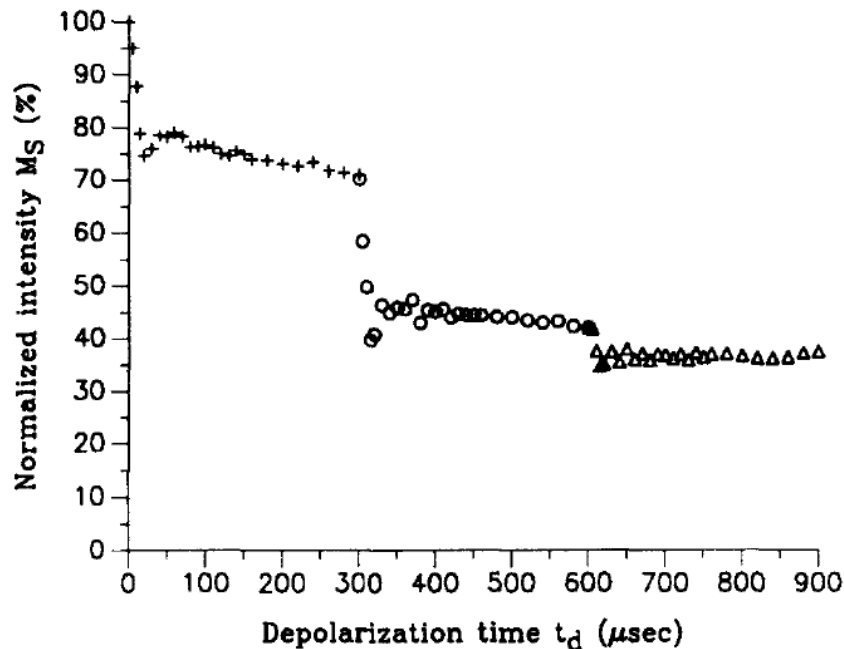


FIG. 7. The depolarization curve for the ^{13}C signal of the sample of $(^{13}\text{CH}_2\text{O})_n$, 96% ^{13}C -enriched, in the modified depolarization experiment. +, Data during $t_d = 0$ to $300 \mu\text{s}$; O, $t_d = 300$ to $600 \mu\text{s}$; Δ , $t_d = 600$ to $900 \mu\text{s}$. The first rapid drop is about 21% of M_0 . The synchronous phase reversals of H_{11} and H_{1S} ($t_d = 300 \mu\text{s}$) result in the second rapid drop of an amount of 24% of M_0 . The second phase reversal ($t_d = 600 \mu\text{s}$) results in a smaller drop of an amount of 6%.

References

1. I. Solomon, Relaxation Processes in a System of 2 Spins, *Physical Review* **99**, 559-565 (1955).
2. J. Jeener, B. H. Meier, P. Bachmann and R. R. Ernst, Investigation of Exchange Processes By 2-Dimensional Nmr- Spectroscopy, *Journal of Chemical Physics* **71**, 4546-4553 (1979).
3. S. Macura and R. R. Ernst, Elucidation of cross relaxation in liquids by two-dimensional N.M.R. spectroscopy (Reprinted from *Molecular Physics*, vol 41, pg 95-117, 1980), *Molecular Physics* **100**, 135-147 (2002).

NMR interactions as tensors: Chemical shielding

When a molecule is placed in a magnetic field shielding currents are induced such that the field the nucleus sees can be written as

$$\vec{B} = \vec{B}_{\text{applied}} (\mathbb{1} - \underline{\underline{\sigma}})$$

where $\mathbb{1} = \begin{pmatrix} 1 & 0 & 0 \\ 0 & 1 & 0 \\ 0 & 0 & 1 \end{pmatrix}$ is a unit matrix and

$\underline{\underline{\sigma}}$ is the shielding tensor. If this is a

Cartesian tensor, expressed in terms of x, y, z lab coordinates we write

$$(\underline{\underline{\sigma}})_{\text{lab}} = \begin{pmatrix} \sigma_{xx} & \sigma_{xy} & \sigma_{xz} \\ \sigma_{yx} & \sigma_{yy} & \sigma_{yz} \\ \sigma_{zx} & \sigma_{zy} & \sigma_{zz} \end{pmatrix}$$

as a matrix we can think of this $\underline{\underline{\sigma}}$ tensor as having been constructed from a pair of vectors $\vec{\sigma}$ (a row vector) and its transpose $\vec{\sigma}^T$ (a column vector) as $\vec{\sigma}^T \cdot \vec{\sigma}$, is a column vector \times a row vector gives a matrix.

In a typical NMR experiment we will put the magnetic field along the z-axis, then

$$\vec{B}_{\text{applied}} = (0, 0, B_0) \text{ and}$$

$$\vec{B} \cdot \underline{\sigma} \approx B_0 \sigma_{zx} \hat{i} + B_0 \sigma_{zy} \hat{j} + B_0 \sigma_{zz} \hat{k}$$

Since the total field is

$$\vec{B} = B_0(1 - \sigma_{zz}) \hat{k} - B_0 \sigma_{zx} \hat{i} - B_0 \sigma_{zy} \hat{j}$$

is to a very good approximation just

$$\vec{B} \approx B_0(1 - \sigma_{zz}) \hat{k}, \text{ we only measure } (\sigma_{zz})_{\text{lab}}$$

As written, σ_{zz} , and $\underline{\sigma}$, are for a particular orientation of the sample in the laboratory frame. If we have a crystal on a goniometer and rotate the sample the components change.

Thus $\underline{\underline{\sigma}}$ as a tensor transforms as

$$\underline{\underline{R}} \cdot \underline{\underline{\sigma}} \cdot \underline{\underline{R}}^{-1}$$

Suppose we rotate the $\underline{\underline{\sigma}}$ tensor about the x-axis by ϕ

$$R_x(\phi) = \begin{pmatrix} 1 & 0 & 0 \\ 0 & \cos\phi & -\sin\phi \\ 0 & \sin\phi & \cos\phi \end{pmatrix}$$

If $(\underline{\underline{\sigma}})_{\text{lab}}^{\phi=0} = (\underline{\underline{\sigma}})_{\text{crystal}}^{\phi=0}$, the new $(\underline{\underline{\sigma}})_{\text{lab}}$ will be a rotated

crystal tensor

$$\begin{aligned} (\underline{\underline{\sigma}})_{\text{lab}} &= R_x(\phi) (\underline{\underline{\sigma}})_{\text{crystal}} R_x^{-1}(\phi) \\ &= \begin{pmatrix} 1 & 0 & 0 \\ 0 & c & -s \\ 0 & s & c \end{pmatrix} \begin{pmatrix} \sigma_{xx} & \sigma_{xy} & \sigma_{xz} \\ \sigma_{yx} & \sigma_{yy} & \sigma_{yz} \\ \sigma_{zx} & \sigma_{zy} & \sigma_{zz} \end{pmatrix} \begin{pmatrix} 1 & 0 & 0 \\ 0 & c & s \\ 0 & -s & c \end{pmatrix} \end{aligned}$$

where we used $c \equiv \cos\phi$, $s \equiv \sin\phi$

$$(\sigma_{zz})_{\text{lab}} = \sin^2 \phi \sigma_{yy} + \cos^2 \phi \sigma_{zz} + \frac{1}{2} \sin 2\phi (\sigma_{zy} + \sigma_{yz})$$

In most circumstances we can assume that

$\underline{\underline{\sigma}}$ is symmetric, i.e. $\sigma_{ij} = \sigma_{ji}$. Furthermore,

the isotropic shift, $\frac{1}{3} \text{Tr} \underline{\underline{\sigma}} = \sigma_{\text{iso}} = \frac{1}{3} (\sigma_{xx} + \sigma_{yy} + \sigma_{zz})$

is invariant to representation, i.e. is a constant

regardless of the frame. We can usually then

assume that $\sigma_{zy} = \sigma_{yz}$ so

$$\left[(\sigma_{zz})_{\text{lab}} \right] = \sin^2 \phi \sigma_{yy} + \cos^2 \phi \sigma_{zz} + \sin 2\phi \sigma_{yz}$$

↑ rotation

If we also perform a y-rotation

$$R_y(\phi) = \begin{pmatrix} \cos \phi & 0 & \sin \phi \\ 0 & 1 & 0 \\ -\sin \phi & 0 & \cos \phi \end{pmatrix}$$

$$\left[(\sigma_{zz})_{\text{lab}} \right] = \sin^2 \phi \sigma_{xx} + \cos^2 \phi \sigma_{zz} - \sin 2\phi \sigma_{zx}$$

y-rotation

now we can rewrite these in the following manner

$$\begin{aligned}
 [\sigma_{zz}(\phi)]_x &= \sin^2 \phi \left(\frac{\sigma_{yy} + \sigma_{zz}}{2} + \frac{\sigma_{yy} - \sigma_{zz}}{2} \right) \\
 &\quad + \cos^2 \phi \left(\frac{\sigma_{yy} + \sigma_{zz}}{2} - \frac{\sigma_{yy} - \sigma_{zz}}{2} \right) \\
 &\quad + \sin 2\phi \sigma_{yz} \\
 &= \frac{\sigma_{yy} + \sigma_{zz}}{2} + \frac{(\sigma_{yy} - \sigma_{zz})}{2} (\sin^2 \phi - \cos^2 \phi) + \sin 2\phi \sigma_{yz} \\
 &= \frac{\sigma_{yy} + \sigma_{zz}}{2} - \frac{(\sigma_{yy} - \sigma_{zz})}{2} \cos 2\phi + \sigma_{yz} \sin 2\phi
 \end{aligned}$$

likewise

$$[\sigma_{zz}(\phi)]_y = \frac{\sigma_{xx} + \sigma_{zz}}{2} - \frac{(\sigma_{xx} - \sigma_{zz})}{2} \cos 2\phi - \sigma_{zx} \sin 2\phi$$

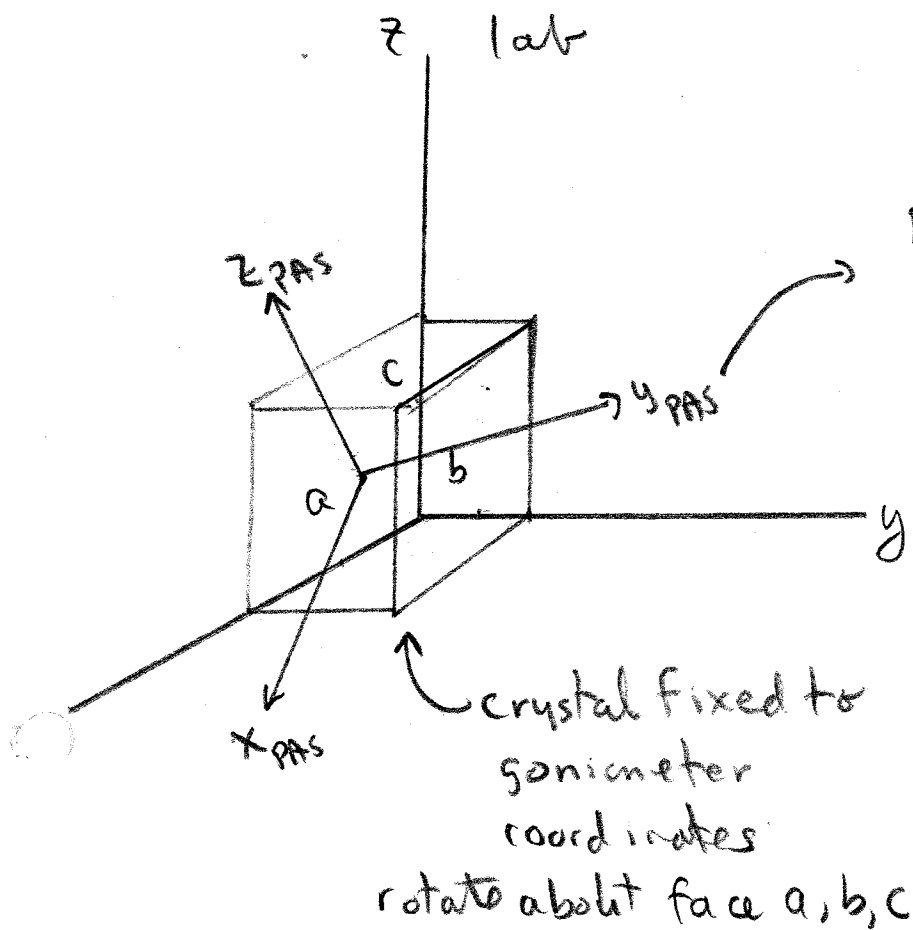
Measuring the isotropic shift $\sigma_{iso} = \frac{1}{3} (\sigma_{xx} + \sigma_{yy} + \sigma_{zz})$ and the 2, ϕ independent terms determines σ_{xx} , σ_{yy} and σ_{zz} . The $\phi = 45^\circ$ orientations then determine σ_{yz} and σ_{xz} . Fits to the curves obtained

determine 5 of the six components. In principle only 2 rot. patterns are needed about axes giving independent results. In practice the x-rotation is first obtained, and the crystal remounted by rotating it 90° in the sample holder to generate a rotation about the $y=y'$ crystal axis. A third reorientation, putting the original crystal axis z' along the lab x axis of the goniometer, yields the final pattern required.

With all 6 independent elements measured the matrix can be diagonalized

$$\begin{pmatrix} \sigma_{xx} & \sigma_{xy} & \sigma_{xz} \\ \sigma_{xy} & \sigma_{yy} & \sigma_{yz} \\ \sigma_{xz} & \sigma_{yz} & \sigma_{zz} \end{pmatrix}_{\text{lab}} \rightarrow \begin{pmatrix} \sigma_{11} & 0 & 0 \\ 0 & \sigma_{22} & 0 \\ 0 & 0 & \sigma_{33} \end{pmatrix}_{\text{PAS}}$$

The eigenvalues are the principal components of the shielding tensor in the principal axis system or PAS. The eigenvectors then relate the PAS to the crystal frame. Knowledge of the molecule's orientation in the crystal allows us to relate the PAS to the molecular frame.



PAS coordinates
Fixed to molecule
 \therefore fixed to
crystal

crystal fixed to
goniometer
coordinates
rotate about face a, b, c

Tensor interactions
and molecular or
mechanical motion

Readings:

Slichter: 279-285

Mehring: 8-14, 288-292

Goldman on rotations

Flygare paper

Spin $\frac{1}{2}$ CSA powder lineshapes and motion

For a spin $\frac{1}{2}$ nucleus with an anisotropic chemical shift, the NMR spectrum is determined by σ_{zz}

$$\nu = -\gamma B_0 (1 - (\sigma_{zz})_{lab}) I_z$$

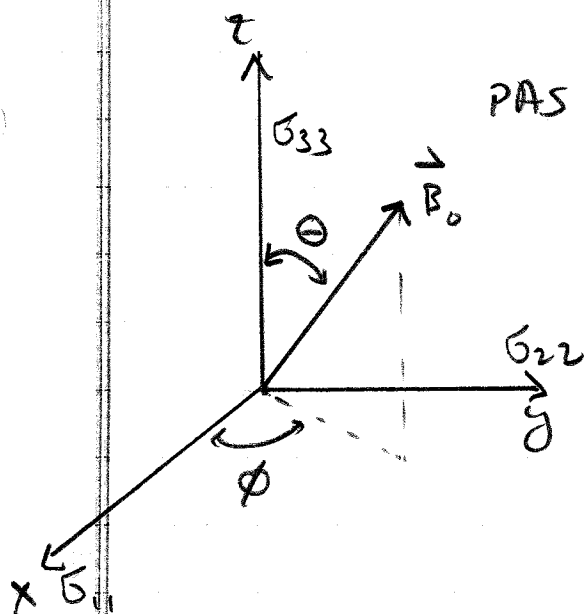
In the PAS the shift tensor may be written

$$\begin{pmatrix} \sigma_{11} & 0 & 0 \\ 0 & \sigma_{22} & 0 \\ 0 & 0 & \sigma_{33} \end{pmatrix}$$

If we write $-\gamma B_0 (1 - \sigma_{ii}) \equiv \nu_{ii}$, the transition frequency along the 3 axes are then ν_{11} , ν_{22} and ν_{33} . Convention often chooses

$$\nu_{11} > \nu_{22} > \nu_{33}$$

although this is not necessary. If the field B_0 is oriented at an angle θ from the z-axis in the PAS, and ϕ is the angle of its projection onto the xy plane from the x-axis,



we can write the anisotropic part as

$$\chi_{\text{CSA}} = \gamma \vec{I} \cdot \underline{\sigma} \cdot \vec{B}$$

keeping only the I_z terms as before, where " I_z " is along \vec{B} , not " z " in the PAS,

$$G_{zz}(\theta, \phi) = \vec{r} \cdot \underline{\sigma} \cdot \vec{b}, \text{ where } \vec{r} \text{ is a unit}$$

vector along \vec{I} , and \vec{b} is a unit vector along \vec{B} . Since we are choosing \vec{r} parallel to \vec{b} , these are the same, and thus

$$G_{zz}(\theta, \phi) = \sigma_{11} \sin^2 \theta \cos^2 \phi + \sigma_{22} \sin^2 \theta \sin^2 \phi + \sigma_{33} \cos^2 \theta$$

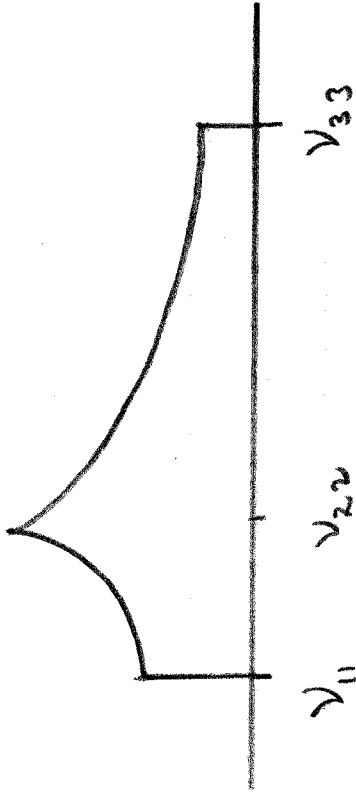
The line shape for a "powder sample", one where all θ & ϕ are possible, with probability $P(\theta, \phi) \propto \sin \theta d\theta d\phi$

is given by the usual formula

$$I(\nu) = \int_0^{2\pi} I(\nu, \phi) d\phi = \int_0^{2\pi} P(\theta) \left(\frac{d\nu}{d\theta} \right)^{-1} d\phi$$

In the general case the line shape is complicated, with intensities proportional to elliptic integrals. More often a powder sum by computer.

is used. The shape qualitatively is as follows



where we have assumed v_{11} is the maximum, v_{33} is the minimum, and v_{22} is the frequency with \vec{B} along the middle axis of the PFS.

An "axially symmetric" shift tensor has 2 components degenerate. For instance if $\sigma_{11} = \sigma_{22} \equiv \sigma_{\perp}$ and $\sigma_{33} \equiv \sigma_{\parallel}$, the σ_{zz} depends only on θ as $\sigma_{zz} = \sigma_{\perp} \sin^2 \theta + \sigma_{\parallel} \cos^2 \theta$ "parallel"

Dipolar couplings under MAS

Under MAS the secular portions of the dipolar interaction will transform as

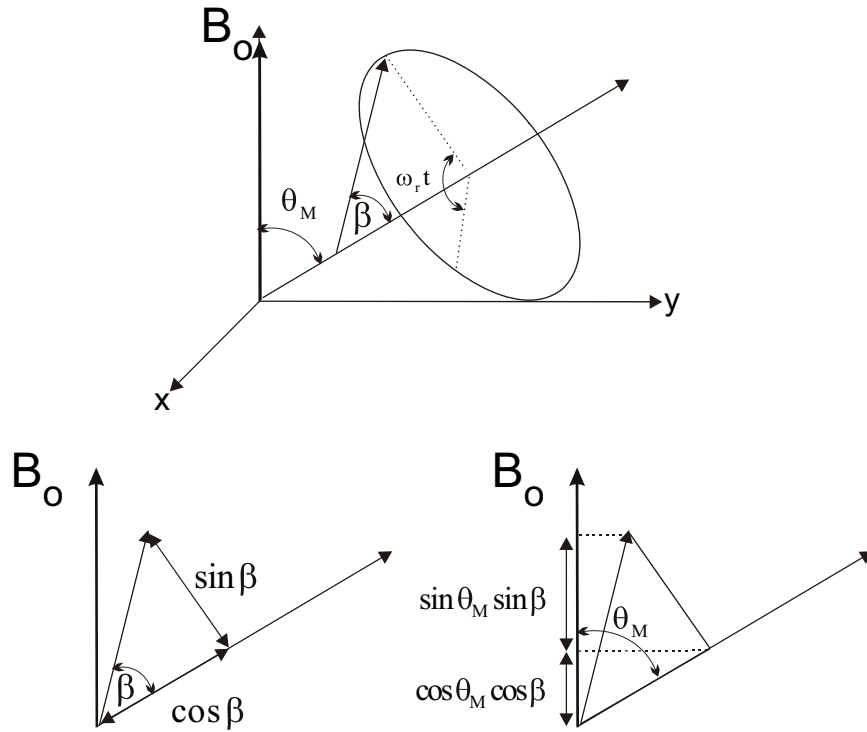
$$D(t) = \bar{r}(t) \cdot \frac{\gamma_1 \gamma_2 \hbar^2}{r^3} \begin{pmatrix} 1 & 0 & 0 \\ 0 & 1 & 0 \\ 0 & 0 & -2 \end{pmatrix} \cdot \bar{r}^T(t)$$

where the dipolar tensor is written in the PAS and $\bar{r}(t)$ is the direction of B_0 in this frame.

Using $\bar{r}(t) = (\sin \theta \cos \varphi, \sin \theta \sin \varphi, \cos \theta)$

$$\begin{aligned} D(t) &= \frac{\gamma_1 \gamma_2 \hbar^2}{r^3} (\sin \theta \cos \varphi, \sin \theta \sin \varphi, \cos \theta) \cdot \begin{pmatrix} 1 & 0 & 0 \\ 0 & 1 & 0 \\ 0 & 0 & -2 \end{pmatrix} \cdot \begin{pmatrix} \sin \theta \cos \varphi \\ \sin \theta \sin \varphi \\ \cos \theta \end{pmatrix} \\ &= \frac{\gamma_1 \gamma_2 \hbar^2}{r^3} (\sin \theta \cos \varphi, \sin \theta \sin \varphi, \cos \theta) \cdot \begin{pmatrix} \sin \theta \cos \varphi \\ \sin \theta \sin \varphi \\ -2 \cos \theta \end{pmatrix} \\ &= \frac{\gamma_1 \gamma_2 \hbar^2}{r^3} (\sin^2 \theta \cos^2 \varphi + \sin^2 \theta \sin^2 \varphi - 2 \cos^2 \theta) \\ &= \frac{\gamma_1 \gamma_2 \hbar^2}{r^3} (\sin^2 \theta - 2 \cos^2 \theta) = \frac{\gamma_1 \gamma_2 \hbar^2}{r^3} (1 - 3 \cos^2 \theta) \end{aligned}$$

If the dipolar unit vector is oriented at an angle β to the spinner axis (set in the yz plane), and it is rotated about the magic angle, it has a time independent component along the axis of $\cos \beta$, and a time dependent component perpendicular to the rotation axis of length $\sin \beta$.



If this component starts out in the yz plane at $t = 0$, it has components of

$$\begin{aligned}
 z &= \sin \beta s \sin \theta_M \cos \omega_r t + \cos \beta s \cos \theta_M \\
 y &= -\sin \beta s \cos \theta_M \cos \omega_r t + \cos \beta s \sin \theta_M \\
 x &= \sin \beta s \sin \omega_r t
 \end{aligned}$$

in a frame with B_0 along the z axis. The hamiltonian requires $1 - 3 \cos^2 \theta(t)$. We can get this from the dot product between the field vector and the dipolar vector. In this instance it is just the z component of the dipolar vector. Thus

$$\begin{aligned}
1 - 3 \cos^2 \theta(t) &= 1 - 3 \left(\sin \beta \sin \theta_M \cos \omega_r t + \cos \beta \cos \theta_M \right)^2 \\
&= 1 - 3 \left(\sin \beta \sqrt{\frac{2}{3}} \cos \omega_r t + \cos \beta \frac{1}{\sqrt{3}} \right)^2 \\
&= 1 - \left(\sqrt{2} \sin \beta \cos \omega_r t + \cos \beta \right)^2 \\
&= 1 - \left(2 \sin^2 \beta \cos^2 \omega_r t + 2\sqrt{2} \sin \beta \cos \beta \cos \omega_r t + \cos^2 \beta \right) \\
&= 1 - \left(\sin^2 \beta (\cos 2\omega_r t + 1) + \sqrt{2} \sin 2\beta \cos \omega_r t + \cos^2 \beta \right) \\
&= 1 - \left(\sin^2 \beta \cos 2\omega_r t + \sqrt{2} \sin 2\beta \cos \omega_r t + \sin^2 \beta + \cos^2 \beta \right) \\
&= 1 - \left(\sin^2 \beta \cos 2\omega_r t + \sqrt{2} \sin 2\beta \cos \omega_r t + 1 \right) \\
&= 1 - 1 - \left(\sin^2 \beta \cos 2\omega_r t + \sqrt{2} \sin 2\beta \cos \omega_r t \right) \\
&= -\sin^2 \beta \cos 2\omega_r t - \sqrt{2} \sin 2\beta \cos \omega_r t
\end{aligned}$$

The standard convention has β as the negative of the angle we defined here. If we let $\omega_r t = \omega_r t' + \gamma$, where γ is the starting phase of the rotation, and set β to $-\beta$ we get the usual result for the secular dipolar hamiltonian of a rotating spin pair under MAS:

$$\begin{aligned}
\mathcal{H}_D &= \frac{\gamma_1 \gamma_2 \hbar^2}{r^3} (1 - 3 \cos^2 \theta(t)) I_Z S_Z \\
&= -\frac{\gamma_1 \gamma_2 \hbar^2}{r^3} I_Z S_Z \left\{ \sin^2 \beta \cos(2\omega_r t + 2\gamma) - \sqrt{2} \sin 2\beta \cos(\omega_r t + \gamma) \right\} \\
&= -D(t) 2I_Z S_Z
\end{aligned}$$

CP and TEDOR transfers

To describe CP and TEDOR transfers under MAS we'll take the dipolar Hamiltonian as

$$\mathcal{H}_D(t) = -D_{IS}(t)2I_zS_z$$

where $D_{IS}(t)$ is given by

$$D_{IS}(t) = D_{IS} \left(\frac{1}{2} \sin^2 \beta \cos(2\omega_r t + 2\gamma) - \frac{1}{\sqrt{2}} \sin 2\beta \cos(\omega_r t + \gamma) \right)$$

CP dynamics

In the double rotating frame (see Wu and Zilm, JMR **104**, 154-165 (1993)) the hamiltonian for an IS spin pair with I and S RF fields has time independent portions given by

$$\begin{aligned} \mathcal{H} = & -\omega_{1I}I_x - \Delta\omega_I I_z - \omega_{1S}S_x \\ & - \Delta\omega_S S_z + 2bI_zS_z + \mathcal{H}_{II}, \quad [1] \end{aligned}$$

where b is usually defined as

$$b = \frac{\gamma_I \gamma_S \hbar}{2r^3} (1 - 3 \cos^2 \theta), \quad [2]$$

Transforming to a doubly tilted rotating frame by rotating about the y axis by the effective field

angles, defined by $\tan \theta_I = \frac{\omega_{1I}}{\Delta\omega_I}$, $\tan \theta_S = \frac{\omega_{1S}}{\Delta\omega_S}$, gives

$$\begin{aligned} \mathcal{H}^T = & -\omega_{eI}I_z - \omega_{eS}S_z + 2bI_xS_x \sin \theta_I \sin \theta_S \\ & + 2bI_zS_z \cos \theta_I \cos \theta_S - 2bI_zS_x \cos \theta_I \sin \theta_S \\ & - 2bI_xS_z \sin \theta_I \cos \theta_S + \mathcal{H}'_{II}, \quad [3] \end{aligned}$$

The effective fields are $\omega_{eI} = \sqrt{\omega_{1I}^2 + \Delta\omega_I^2}$ and $\omega_{eS} = \sqrt{\omega_{1S}^2 + \Delta\omega_S^2}$. Close to resonance we have

$$\mathcal{H}^T = -\omega_{eI}I_z - \omega_{eS}S_z + 2b \sin \theta_I \sin \theta_S (I_x S_x). \quad [4]$$

since then $\theta_I \approx \theta_S \approx 90^\circ$. We can simply use the on-resonance hamiltonian

$$\mathcal{H}^T = -\omega_{1I}I_z - \omega_{1S}S_z + 2bI_xS_x, \quad [5]$$

and recognize any result can be made valid for small resonance offsets by scaling b by $\sin\theta_I \sin\theta_S$ and using the effective fields in place of the RF field amplitudes. Under MAS we can rewrite $\mathcal{H}_D(t)$ as before substituting $D_{IS}(t)$ for b

$$\mathcal{H}_D(t) = 2D_{IS}(t)I_xS_x$$

Notice the transformation has just put the z-axis along the spin locking field, in essence permuting x and z in equation 1. The problem is simpler recasting the hamiltonian in terms of single transition operators as

$$\mathcal{H}^T = -\Delta I_z^{23} - \Sigma I_z^{14} + b(I_x^{14} + I_x^{23}), \quad [6]$$

where

$$\Delta = \omega_{1I} - \omega_{1S}, \quad \Sigma = \omega_{1I} + \omega_{1S}$$

And the single transition operators are defined

$$\begin{aligned} I_z^{23} &= \frac{I_z - S_z}{2}, & I_z^{14} &= \frac{I_z + S_z}{2}, \\ I_x^{14} &= \frac{I_+S_+ + I_-S_-}{2}, & I_x^{23} &= \frac{I_+S_- + I_-S_+}{2}. \end{aligned} \quad [7]$$

The 14 operators correspond to the sum magnetization, i.e. $I_z^{14} = \frac{I_z + S_z}{2}$, whereas the 23 subspace is for the difference polarization. The hamiltonian in the product basis is

$$\begin{array}{c}
|++\rangle \quad |--\rangle \quad |+-\rangle \quad |-+\rangle \\
\begin{array}{|c|c|c|c|}
\hline
\langle 4| & -\Sigma/2 & b/2 & \\
\hline
\langle 1| & b/2 & \Sigma/2 & \\
\hline
\langle 2| & & & -\Delta/2 & b/2 \\
\hline
\langle 3| & & & b/2 & \Delta/2 \\
\hline
\end{array}
\end{array} \quad [8]$$

where the correspondence $|++\rangle = |4\rangle$, $|--\rangle = |1\rangle$, $|+-\rangle = |2\rangle$, $|-+\rangle = |3\rangle$ is made. The hamiltonian consists of two pieces, one confined to the 14 subspace and the other to the 23 subspace, and thus these pieces evolve independently. As long as $b \ll \Sigma$, evolution takes place solely in the 23 space, and the sum magnetization is a constant of the motion.

In this case the 23 space can be represented by a set of effective pseudo spin 1/2 operators of the form

$$\mathcal{H}^{23} = -a(t) I_z^{23} + b(t) I_x^{23} \quad [9]$$

The $-a(t)$ factor is the "resonance offset" while $b(t)$ plays the role of the RF field. The dipolar coupling $b(t)$ can be expanded in Fourier components in the usual way:

$$\begin{aligned}
b(t) &= \sum_{k=-2}^2 b_k e^{ik\omega_r t}, \quad \text{where} \\
b_{\pm 1} &= -D_{IS} \frac{\sqrt{2}}{4} \sin(2\beta) e^{\pm iy}, \quad b_{\pm 2} = -D_{IS} \frac{1}{4} \sin^2 \beta e^{\pm 2iy}
\end{aligned} \quad [10]$$

and

$$D_{IS} = \frac{\mu_o}{4\pi} \frac{\gamma_I \gamma_S \hbar}{r^3} \text{ (rad s}^{-1}\text{)}$$

If we transform hamiltonian to a frame rotating about z in the 23 subspace at a frequency close to either $\pm\omega_r$ or $\pm 2\omega_r$, one term in $b(t)$ will become slowly varying and dominate the evolution.

This portion can be written as

$$\mathcal{H}^{23} = \text{Re}(b_k) I_x^{23} - \text{Im}(b_k) I_y^{23} - (\Delta - k\omega_r) I_z^{23} \quad [11]$$

When Δ is set to $\pm\omega_r$ or $\pm 2\omega_r$, we have an "on resonance" effective hamiltonian, which we can rewrite as

$$I_z^{23} = -D_k \left(I_x^{23} \cos \gamma - I_y^{23} \sin \gamma \right) \quad [12]$$

where k is either 1 or 2, and we have defined the terms D_1 and D_2 as

$$D_1 = D_{IS} \frac{\sqrt{2}}{4} \sin 2\beta \quad \text{and} \quad D_2 = D_{IS} \frac{1}{4} \sin^2 \beta$$

The evolution is simple in this case. The initial spin locked magnetization represents a density operator proportional to I_z^{23} . We then have a simple rotation of I_z^{23} by an effective "RF" field with a phase of γ . Since the z-component at anytime is independent of the phase, the magnetization transfer is independent of γ , or as it is sometimes called " γ -encoded". The resulting transfer is found from

$$I_z^{23}(t) = I_z^{23}(0) \cos(-D_k t) = \frac{1}{2} I_z(0) \cos(-D_k t)$$

where the last step follows if there is no initial S-spin magnetization spin locked. Since I_z^{14} is independent of time, it follows using $I_z^{14} = \frac{I_z + S_z}{2} = \frac{1}{2} I_z(0)$ that

$$S_z(t) = I_z^{14}(t) - I_z^{23}(t) = \frac{1}{2} I_z(0) (1 - \cos D_k t) = I_z(0) \sin^2 \left(\frac{1}{2} D_k t \right)$$

Returning to the usual rotating frame, we now write the magnetization in phase with an x-phase spin locking field after CP at the $k = \pm 1$ sideband match as

$$S_x(t) = I_z(0) \sin^2 \left\{ \left(D_{IS} \frac{\sqrt{2}}{8} \sin 2\beta \right) t \right\}$$

while at the $k = \pm 2$ sideband match we get

$$S_x(t) = I_z(0) \sin^2 \left\{ \left(D_{IS} \frac{1}{8} \sin^2 \beta \right) t \right\}$$

Off any of the matching conditions the result is also a simple rotation of the initial state about the effective field. Close to the k match we have

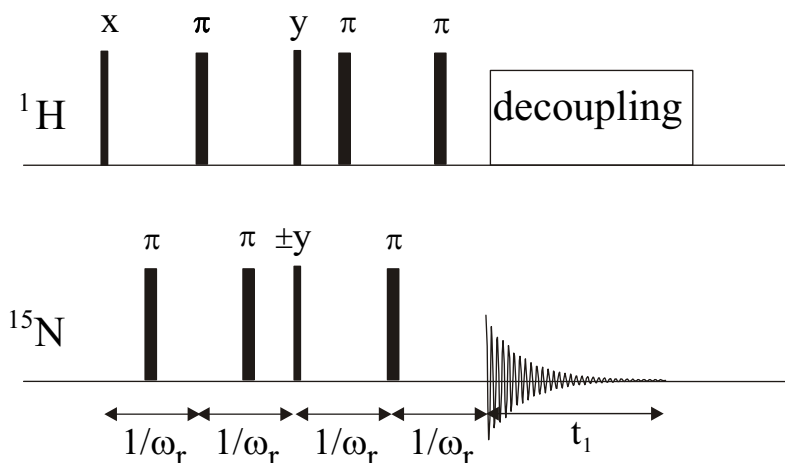
$$S_x(t) = \frac{|b_k|^2}{|b_k|^2 + (\Delta - k\omega_r)^2} I_z(0) \sin^2 \left\{ \frac{1}{2} \sqrt{|b_k|^2 + (\Delta - k\omega_r)^2} t \right\}$$

We see the departure of the modified Hartmann-Hahn match plays the role of an off-resonance detuning, while the dipolar coupling acts as an RF field. Since this field depends on β the transfer is heterogeneous.

An adiabatic CP transfer works just like an adiabatic inversion, and in the limit of true adiabaticity provides for a complete β independent transfer from one spin to another. The idea in an adiabatic following is to start very far off-resonance, in this case very far from the Hartmann-Hahn match. As the match condition is adiabatically varied through "resonance", the magnetization follows the effective field and adiabatically inverts, even for a wide spread of field strengths, i.e. dipolar couplings.

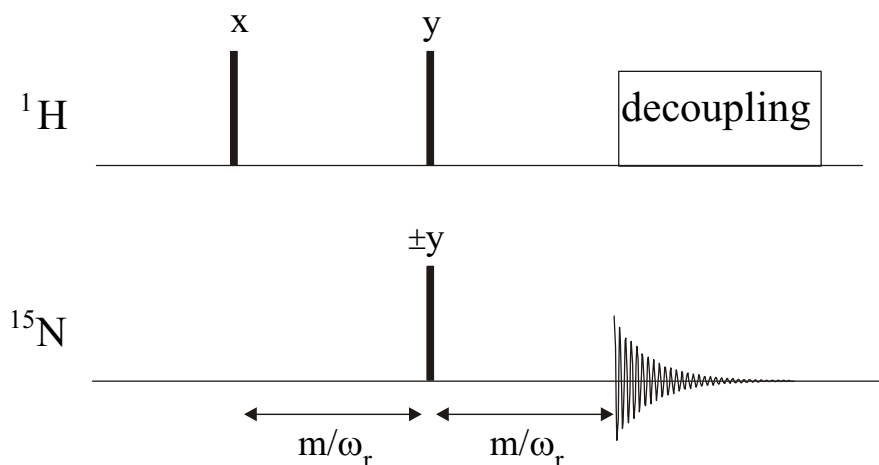
TEDOR transfers

A chemical shift compensated TEDOR sequence appropriate for ^1H - ^{15}N transfers is shown below



The first pair of $1/\omega_r$ intervals takes the ^1H transverse magnetization created by the first ^1H $\pi/2$ pulse and dephases it with a REDOR sequence. The π pulses are set so as to refocus the ^1H isotropic chemical shift and not recouple the ^1H anisotropic shift. The pair of $\pi/2$ y pulses converts the anti-phase ^1H magnetization created this way into anti-phase ^{15}N magnetization. The second pair of $1/\omega_r$ intervals rephases this, again using REDOR, and with the π pulses placed so as to refocus the ^{15}N chemical shift.

The evolution of the magnetization in this sequence can be represented by the following generic sequence, where the spins evolve during the m/ω_r intervals under an average hamiltonian



with no chemical shifts, but with a REDOR recoupled heteronuclear dipolar term.

In describing TEDOR for an IS spin pair it is most convenient to first calculate the average of the dipolar Hamiltonian over a rotor period. This is simple since the heteronuclear dipolar and anisotropic chemical shift interactions commute with each other and themselves at all times. We will denote the average as $\bar{\mathcal{H}}_D = -\bar{D}_{IS}(t)2I_zS_z$ where we calculate \bar{D}_{IS} as

$$\bar{D}_{IS} = D_{IS} \frac{1}{\tau_r} \left\{ \int_0^{\tau_1} \left[\frac{1}{2} \sin^2 \beta \cos(2\omega_r t + 2\gamma) - \frac{1}{\sqrt{2}} \sin 2\beta \cos(\omega_r t + \gamma) \right] dt - \int_{\tau_1}^{\tau_2} [] dt + \dots + \int_{\tau_{n-1}}^{\tau_n} [] dt \right\}$$

The different intervals $\tau_j - \tau_i$ represent the periods where dipolar interaction freely evolves under MAS. At the different times τ the sign is changed by application of a π pulse to one of the spins in the IS pair. The resulting dipolar Hamiltonian can then be used to evaluate the evolution at multiples of a rotor period using the product operator formalism.

We want to consider two different situations which we will call 1/2 and 1/4 TEDOR, where the designation signifies the fraction of a rotor period between successive π pulses. In TEDOR_{1/2} we have a single π in the middle of rotor period. In each case we basically need the following integrals of the $\cos(2\omega_r t + 2\gamma)$ and $\cos(\omega_r t + \gamma)$ functions:

TEDOR_{1/2}

The $\cos 2\omega_r t$ term gives:
$$\frac{1}{\tau_r} \left\{ \int_{t'}^{t'+\tau_r/2} \cos(2\omega_r t + 2\gamma) dt - \int_{t'+\tau_r/2}^{t'+\tau_r} \cos(2\omega_r t + 2\gamma) dt \right\} = 0$$

While the $\cos \omega_r t$ terms reduces to:

$$\begin{aligned} \frac{1}{\tau_r} \left\{ \int_{t'}^{t'+\tau_r/2} \cos(\omega_r t + \gamma) dt - \int_{t'+\tau_r/2}^{t'+\tau_r} \cos(\omega_r t + \gamma) dt \right\} &= \frac{1}{\omega_r \tau_r} \left\{ \sin(\omega_r t + \gamma) \Big|_{t'}^{t'+\tau_r/2} - \sin(\omega_r t + \gamma) \Big|_{t'+\tau_r/2}^{t'+\tau_r} \right\} \\ &= -\frac{2}{\pi} \sin(\omega_r t' + \gamma) \end{aligned}$$

TEDOR_{1/4}

The $\cos \omega_r t$ term averages as

$$\frac{1}{\tau_r} \left\{ \int_{t'}^{t'+\tau_r/4} \cos(\omega_r t + \gamma) dt - \int_{t'+\tau_r/4}^{t'+\tau_r/2} \cos(\omega_r t + \gamma) dt + \int_{t'+\tau_r/2}^{t'+3\tau_r/4} \cos(\omega_r t + \gamma) dt - \int_{t'+3\tau_r/4}^{t'+\tau_r} \cos(\omega_r t + \gamma) dt \right\} = 0$$

and the $2\omega_r t$ terms gives

$$\begin{aligned} &\frac{1}{\tau_r} \left\{ \int_{t'}^{t'+\tau_r/4} \cos(2\omega_r t + 2\gamma) dt - \int_{t'+\tau_r/4}^{t'+\tau_r/2} \cos(2\omega_r t + 2\gamma) dt + \int_{t'+\tau_r/2}^{t'+3\tau_r/4} \cos(2\omega_r t + 2\gamma) dt - \int_{t'+3\tau_r/4}^{t'+\tau_r} \cos(2\omega_r t + 2\gamma) dt \right\} \\ &= \frac{1}{2\omega_r \tau_r} \left\{ \sin(2\omega_r t + 2\gamma) \Big|_{t'}^{t'+\tau_r/4} - \sin(2\omega_r t + 2\gamma) \Big|_{t'+\tau_r/4}^{t'+\tau_r/2} + \sin(2\omega_r t + 2\gamma) \Big|_{t'+\tau_r/2}^{t'+3\tau_r/4} - \sin(2\omega_r t + 2\gamma) \Big|_{t'+3\tau_r/4}^{t'+\tau_r} \right\} \\ &= \frac{1}{4\pi} \left\{ 2 \sin(2\omega_r t' + 2\gamma + \pi) - \sin(2\omega_r t + 2\gamma) - 2 \sin(2\omega_r t' + 2\gamma + 2\pi) \right. \\ &\quad \left. + 2 \sin(2\omega_r t' + 2\gamma + 3\pi) - \sin(2\omega_r t' + 2\gamma + 4\pi) \right\} \\ &= \frac{1}{4\pi} \left\{ -2 \sin(2\omega_r t' + 2\gamma) - 2 \sin(2\omega_r t' + 2\gamma) - 2 \sin(2\omega_r t' + 2\gamma) - 2 \sin(2\omega_r t' + 2\gamma) \right\} \\ &= \frac{1}{4\pi} \left\{ -8 \sin(2\omega_r t' + 2\gamma) \right\} = -\frac{2}{\pi} \sin(2\omega_r t' + 2\gamma) \end{aligned}$$

For the two cases then we have for \bar{D}_{IS} using

$$D_{IS}(t) = D_{IS} \left(\frac{1}{2} \sin^2 \beta \cos(2\omega_r t + 2\gamma) - \frac{1}{\sqrt{2}} \sin 2\beta \cos(\omega_r t + \gamma) \right), \text{ then}$$

$$\bar{D}_{IS1/2} = -\frac{2}{\pi} \sin(\omega_r t' + \gamma) \left(-D_{IS} \frac{1}{\sqrt{2}} \sin 2\beta \right) = \frac{D_{IS}}{\pi} \sqrt{2} \sin 2\beta \sin(\omega_r t' + \gamma)$$

$$\bar{D}_{IS1/4} = -\frac{2}{\pi} \sin(2\omega_r t' + 2\gamma) \left(D_{IS} \frac{1}{2} \sin^2 \beta \right) = -\frac{D_{IS}}{\pi} \sin^2 \beta \sin(2\omega_r t' + 2\gamma)$$

We can then also rewrite $\bar{\mathcal{R}}_D = -\bar{D}_{IS}(t) 2I_z S_z$ as $\bar{\mathcal{R}}_D = Q_n I_z S_z$ where

$$Q_{1/2} = -2\bar{D}_{IS1/2} = -D_{IS} \frac{2\sqrt{2}}{\pi} \sin 2\beta \sin(\omega_r t' + \gamma)$$

$$Q_{1/4} = -2\bar{D}_{IS1/4} = D_{IS} \frac{2}{\pi} \sin^2 \beta \sin(2\omega_r t' + 2\gamma)$$

where the subscripts are for the 1st type of REDOR (π each $1/2 \tau_r$) and the 2nd type (π each $1/4 \tau_r$).

Propagators

In each of these cases we have a propagator that is of the form (assuming for example that all π pulses are applied to the I spin) :

TEDOR_{1/2}

$$e^{-i\pi I_x} e^{-i\mathcal{R}_D \tau_2} e^{-i\pi I_x} e^{-i\mathcal{R}_D \tau_1} = e^{-i\pi I_x} \left(e^{-i\pi I_x} e^{+i\pi I_x} \right) e^{-i\mathcal{R}_D \tau_2} e^{-i\pi I_x} e^{-i\mathcal{R}_D \tau_1} = e^{-i\pi I_x} e^{-i\pi I_x} e^{+i\mathcal{R}_D \tau_2} e^{-i\mathcal{R}_D \tau_1} = e^{-i\bar{\mathcal{R}}_D (\tau_1 + \tau_2)}$$

TEDOR_{1/4}

$$\begin{aligned} e^{-i\pi I_x} e^{-i\mathcal{R}_D \tau_4} e^{-i\pi I_x} e^{-i\mathcal{R}_D \tau_3} e^{-i\pi I_x} e^{-i\mathcal{R}_D \tau_2} e^{-i\pi I_x} e^{-i\mathcal{R}_D \tau_1} &= e^{-i\pi I_x} e^{-i\mathcal{R}_D \tau_4} e^{-i\pi I_x} e^{-i\mathcal{R}_D \tau_3} e^{-i\pi I_x} \left(e^{-i\pi I_x} e^{+i\pi I_x} \right) e^{-i\mathcal{R}_D \tau_2} e^{-i\pi I_x} e^{-i\mathcal{R}_D \tau_1} \\ &= e^{-i\pi I_x} \left(e^{-i\pi I_x} e^{+i\pi I_x} \right) e^{-i\mathcal{R}_D \tau_4} e^{-i\pi I_x} e^{-i\mathcal{R}_D \tau_3} e^{+i\mathcal{R}_D \tau_2} e^{-i\mathcal{R}_D \tau_1} = e^{-i\pi I_x} \left(e^{-i\pi I_x} e^{+i\pi I_x} \right) e^{-i\mathcal{R}_D \tau_4} e^{-i\pi I_x} e^{-i\mathcal{R}_D \tau_3} e^{+i\mathcal{R}_D \tau_2} e^{-i\mathcal{R}_D \tau_1} \\ &= e^{-i\pi I_x} e^{-i\pi I_x} e^{+i\mathcal{R}_D \tau_4} e^{-i\mathcal{R}_D \tau_3} e^{+i\mathcal{R}_D \tau_2} e^{-i\mathcal{R}_D \tau_1} \\ &= e^{+i\mathcal{R}_D \tau_4} e^{-i\mathcal{R}_D \tau_3} e^{+i\mathcal{R}_D \tau_2} e^{-i\mathcal{R}_D \tau_1} = e^{-i\bar{\mathcal{R}}_D (\tau_1 + \tau_2 + \tau_3 + \tau_4)} \end{aligned}$$

Heteronuclear shift correlation, INEPT transfer
and Product Operators - Sorensen/Ernst paper
Goldman, Ch. 6

In addition to chemical exchange and cross-relaxation, magnetization can be transferred between spins via scalar couplings.

Longitudinal magnetization can be exchanged by flip-flip operators. Thus difference z -magnetization evolves under dipolar mediated cross-relaxation

$(I_z - S_z) \rightarrow$ equilibrates with $I_+S_- + I_-S_+$

or terms like I_xS_x . Transverse magnetization

$(I_x - S_x)$ likewise is affected by I_zS_z terms, since if we relabel the axes $x \rightarrow z$ and $z \rightarrow x$ we get the same situation.

Evolution under \mathcal{H} and J

For a pair of spins in the X -approximation, we can write the rotating frame Hamiltonian as

$$\mathcal{H} = \omega_I I_z + \omega_S S_z + 2\pi J I_z S_z$$

where we are in a doubly rotating frame ($U = e^{i(\omega_I I_z + \omega_S S_z)t}$) and all signs have been absorbed into ω_I, ω_S and J to be

dealt with later. Evolution of ρ under this follows

$$\rho(t) = e^{-i(\omega_I I_z + \omega_S S_z + 2\pi J I_z S_z)t} \rho(0) e^{+i(\omega_I I_z + \omega_S S_z + 2\pi J I_z S_z)t}$$

$$= \left[e^{-i\omega_I I_z t} e^{-i\omega_S S_z t} e^{-i2\pi J I_z S_z t} \right] \rho(0) \times \left[e^{+i2\pi J I_z S_z t} e^{+i\omega_S S_z t} e^{+i\omega_I I_z t} \right]$$

which follows from $[I_z, S_z] = 0$ and $[I_z, I_z S_z] = 0$, etc.

We know how to deal with $e^{-i\theta I_z} \hat{p} e^{+i\theta I_z}$

if \hat{p} is a linear combination of I_x, I_y and I_z from

$$e^{-i\theta \hat{A}} \hat{B} e^{i\theta \hat{A}} = \hat{B} \cos \theta + i [\hat{B}, \hat{A}] \sin \theta$$

J-evolution - the bilinear $(I_z S_z)$ rotation

is only slightly more complex. For instance

$$e^{-i(J2\pi S_z t) I_z} I_x e^{+i(J2\pi S_z t) I_z}$$

$$= I_x \cos(2\pi J S_z t) + i [I_x, I_z] \sin(2\pi J S_z t)$$

which follows from setting $2\pi J \hat{S}_z t \equiv \theta$ above, and recognizing that \hat{S}_z , although an operator

has no effect on \hat{I}_z , and thus can be treated as a number. The usual rules apply for our rotations, therefore calling

$$\theta_J = 2\pi J S_z t$$

$$e^{-i\theta_J t} I_z e^{i\theta_J t} = I_z$$

$$e^{-i\theta_J t} I_x e^{i\theta_J t} = I_x \cos(2\pi J S_z t) + I_y \sin(2\pi J S_z t)$$

$$e^{-i\theta_J t} I_y e^{i\theta_J t} = I_y \cos(2\pi J S_z t) - I_x \sin(2\pi J S_z t)$$

These results are general, but the terms

$\cos(2\pi J S_z t)$ and $\sin(2\pi J S_z t)$
are cumbersome.

Product Operators and Spin $\frac{1}{2}$

For an n -spin system, the density matrix can be thought of as a combination of product operators

$$I_{\alpha_1} I_{\beta_2} I_{\delta_3} \dots$$

$$\alpha, \beta, \delta = x, y, z$$

$$1, 2, 3 = \text{spin numbers}$$

as such operators represent all possible matrix elements. Most often we define operators

with respect to a convenient basis set, in NMR this is the familiar product basis. Single transition operators can be defined for a pair of states $|k\rangle$ and $|r\rangle$ as

$$I_{kr} = |k\rangle\langle r| \text{ since the matrix elements in}$$

this basis $\langle m|I_{kr}|n\rangle = \langle m|k\rangle\langle r|n\rangle = \delta_{mk}\delta_{rn}$

or, in other words, are zero for all combinations except $\langle k|I_{kr}|r\rangle = 1$.

Another useful trick is to recognize that any two operators that have the same matrix elements must be the same. For instance we know

$$\hat{I}^2 \equiv \hat{I} \cdot \hat{I} = \hat{I}_x^2 + \hat{I}_y^2 + \hat{I}_z^2 \text{ operates on}$$

" \rightarrow "
meas operator

an angular momentum function $|I, m\rangle$

$I =$ total spin, $m = z$ -projection, as

$$\hat{I}^2 |I, m\rangle = I(I+1) |I, m\rangle$$

We can use $I(I+1) = I^2 + I$ as equivalent to I^2

since the matrix elements are the same. Since

$I(I+1)$ is a number, it commutes with all operators and never produces any evolution of β .

This idea can be extended to spin $\frac{1}{2}$ operators.

In the usual $\{|\frac{1}{2}\rangle, |-\frac{1}{2}\rangle\} \sim \{|+\rangle, |-\rangle\}$ basis

$$\hat{I}_z = \frac{1}{2} \begin{pmatrix} 1 & 0 \\ 0 & -1 \end{pmatrix} \quad \hat{I}_x = \frac{\hat{I}_+ + \hat{I}_-}{2} = \frac{1}{2} \begin{pmatrix} 0 & 1 \\ 1 & 0 \end{pmatrix}$$

$$\hat{I}_y = \frac{\hat{I}_+ - \hat{I}_-}{2i} = \frac{1}{2i} \begin{pmatrix} 0 & 1 \\ -1 & 0 \end{pmatrix}$$

From this we see that $\hat{I}_z^2 = \frac{1}{4} \begin{pmatrix} 1 & 0 \\ 0 & -1 \end{pmatrix} \begin{pmatrix} 1 & 0 \\ 0 & -1 \end{pmatrix} = \frac{1}{4} \begin{pmatrix} 1 & 0 \\ 0 & 1 \end{pmatrix}$

But the number operator $\frac{1}{4}$ has the same elements

$$\frac{1}{4} = \begin{pmatrix} \frac{1}{4} & 0 \\ 0 & \frac{1}{4} \end{pmatrix}, \text{ thus } \hat{I}_z^2 = \frac{1}{4}, \text{ for spin } \frac{1}{2},$$

This is simply overstating that the only values

I_z has are $\frac{1}{2}$ and $-\frac{1}{2}$, and their squares are always $\frac{1}{4}$.

likewise we have

$$I_z I_x = \frac{1}{4} \begin{pmatrix} 1 & 0 \\ 0 & -1 \end{pmatrix} \begin{pmatrix} 0 & 1 \\ 1 & 0 \end{pmatrix} = \frac{1}{4} \begin{pmatrix} 0 & 1 \\ -1 & 0 \end{pmatrix} = \frac{1}{2} (i) (\hat{I}_y)$$

$$I_x I_z = \frac{1}{4} \begin{pmatrix} 0 & 1 \\ 1 & 0 \end{pmatrix} \begin{pmatrix} 1 & 0 \\ 0 & -1 \end{pmatrix} = \frac{1}{4} \begin{pmatrix} 0 & -1 \\ 1 & 0 \end{pmatrix} = -\frac{1}{2} (i) (\hat{I}_y)$$

so

$$[I_z, I_x] = i \left(\frac{I_y}{2} - \left(-\frac{I_y}{2} \right) \right) = i I_y \text{ as expected}$$

$$I_x^2 = \frac{1}{4} \begin{pmatrix} 0 & 1 \\ 1 & 0 \end{pmatrix} \begin{pmatrix} 0 & 1 \\ 1 & 0 \end{pmatrix} = \frac{1}{4} \begin{pmatrix} 1 & 0 \\ 0 & 1 \end{pmatrix} = \frac{1}{4} \text{ also}$$

This approach can be used to simplify

$$\cos(2\pi J S_z t) \text{ and } \sin(2\pi J S_z t),$$

Remembering $\cos(x) = 1 - \frac{1}{2!} x^2 + \frac{1}{4!} x^4 - \dots$

$$\sin(x) = x - \frac{1}{3!} x^3 + \frac{1}{5!} x^5 - \dots$$

$$\cos(2\pi J t S_z) = \cos(\theta S_z)$$

$$= 1 - \frac{\theta^2}{2!} S_z^2 + \frac{\theta^4}{4!} S_z^4 - \dots$$

$$\text{since } (\hat{S}_z)^{2n} = \left(\frac{1}{4}\right)^n = \left(\frac{1}{2}\right)^{2n}$$

$$\begin{aligned} \cos(2\pi Jt S_z) &= 1 - \frac{1}{2!} \left(\frac{\theta}{2}\right)^2 + \frac{1}{4!} \left(\frac{\theta}{4}\right)^4 - \dots \\ &= \cos(\pi Jt) \end{aligned}$$

likewise

$$\sin(2\pi Jt S_z) = \theta S_z - \frac{1}{3!} (\theta S_z)^3 + \frac{1}{5!} (\theta S_z)^5 - \dots$$

$$\text{Since } \hat{S}_z^2 = \frac{1}{4}, \quad 4S_z^2 = 1$$

$$\begin{aligned} \sin(2\pi Jt S_z) &= 4S_z^2 \left(\theta S_z - \frac{1}{3!} (\theta S_z)^3 + \frac{1}{5!} (\theta S_z)^5 - \dots \right) \\ &= 2S_z \left(\theta (2S_z^2) - \frac{1}{3!} \theta^3 (2S_z^4) + \frac{1}{5!} \theta^5 (2S_z^6) - \dots \right) \\ &= 2S_z \left(\theta \left(2 \cdot \frac{1}{4}\right) - \frac{1}{3!} \theta^3 \left(2 \cdot \frac{1}{4^2}\right) + \frac{1}{5!} \theta^5 \left(2 \cdot \frac{1}{4^3}\right) - \dots \right) \\ &= 2S_z \left(\frac{\theta}{2} - \frac{1}{3!} \left(\frac{\theta}{2}\right)^3 + \frac{1}{5!} \left(\frac{\theta}{2}\right)^5 - \dots \right) \\ &= 2S_z \sin\left(\frac{\theta}{2}\right) = 2S_z \sin(\pi Jt) \end{aligned}$$

So for spin $\frac{1}{2}$

$$e^{-i2\pi J S_z I_z t} I_x e^{i2\pi J S_z I_z t}$$

$$= I_x \cos(\pi J t) + I_y (2S_z \sin(\pi J t))$$

and

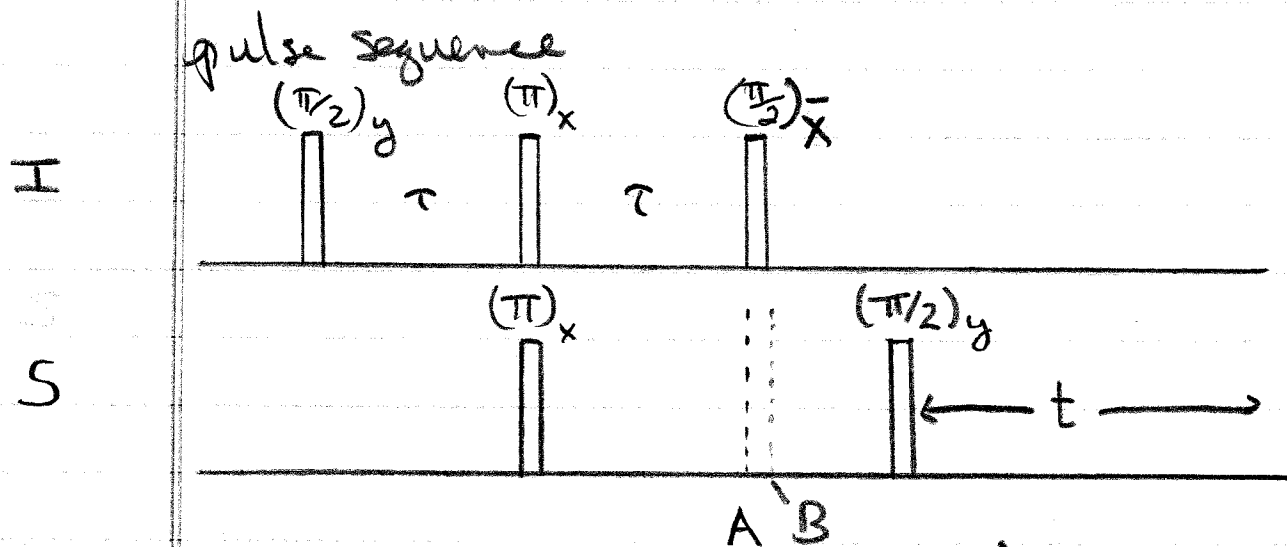
$$e^{-i2\pi J S_z I_z t} I_y e^{i2\pi J S_z I_z t}$$

$$= I_y \cos(\pi J t) - I_x (2S_z \sin(\pi J t))$$

spin $\frac{1}{2}$

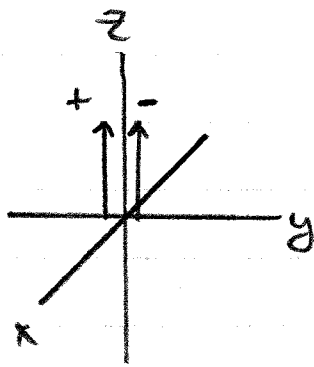
only!

INEPT transfers consider the following



Up to the last 2 pulses (point A), this is just the spin echo we used on page 85-87 to do spectral editing.

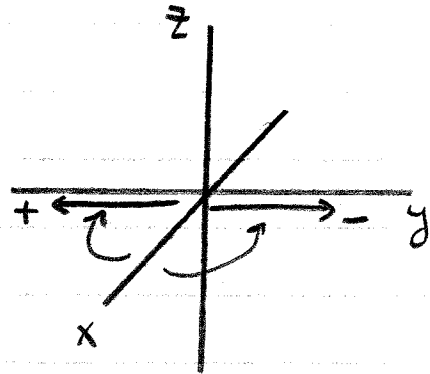
If we have a 2 spin system, both spin $\frac{1}{2}$, pictorially we know that the spin follow a trajectory determined by J , and that all chemical shifts are refocused.



I spin magnetization

$$2\tau = \frac{1}{2J}$$

$$\tau = \frac{1}{4J}$$



"anti-phase" transverse magnetization

M_z for I with $S_{in} \rightarrow$

$$\left\{ \begin{array}{l} \frac{1 - \frac{\delta_I}{2} - \frac{\delta_S}{2}}{1 \rightarrow \rightarrow} \textcircled{4} \quad \frac{V_I + V_S + J}{2} \\ \frac{1 + \frac{\delta_I}{2} - \frac{\delta_S}{2}}{1 \rightarrow \rightarrow} \textcircled{3} \quad \frac{-V_I + V_S - J}{2} \end{array} \right\} V_I + \frac{J}{2}$$

V_I

$$\left\{ \begin{array}{l} \frac{+V_S - V_S - J}{2} \quad \frac{1 - \frac{\delta_I}{2} + \frac{\delta_S}{2}}{1 \rightarrow \rightarrow} \textcircled{2} \\ \frac{-V_S - V_I + J}{2} \quad \frac{1 + \frac{\delta_I}{2} + \frac{\delta_S}{2}}{1 \rightarrow \rightarrow} \textcircled{1} \end{array} \right\} M_z \text{ for I with } S_{in} \rightarrow$$

at point "A" if we apply a $(\frac{\pi}{2})_x^I$ pulse, the \leftarrow vector goes back up along z , while the \rightarrow vector goes to $-z$. This inverts the populations of levels ③ and ④ while leaving those of ① and ② alone. The S-spin transitions now have different starting population differences. Comparing

transition	S_z at $t=0$	S_z at $t=A+$
$1 \rightarrow 3$	$\nu_S - \frac{J}{2}$	$\delta_I - \delta_S$
$2 \rightarrow 4$	$\nu_S + \frac{J}{2}$	$-\delta_I - \delta_S$

The S-spin signal now knows about the I-spin magnetization. This is straight-forward to analyse using product-operators.

Product Operator analysis of INEPT

We take $\rho(0) = a I_z + b S_z$ where

$a = \frac{\gamma_I B_0 h}{kT}$ and $b = \frac{\gamma_S B_0 h}{kT}$ are the appropriate

Boltzmann factors in the high temperature limit.

Using the commutation properties as before

$$\rho(2\tau) = \left\{ e^{-i(\gamma_J + \gamma_S)\tau} e^{-i\pi S_x} e^{-i\pi I_x} e^{-i(\gamma_J + \gamma_S)\tau} \right\} \\ \times e^{-i\frac{\pi}{2} I_y} \hat{\rho}(0) e^{i\frac{\pi}{2} I_y} \left\{ \right\}^*$$

$$= \left\{ e^{-i(\gamma_J + \gamma_S)\tau} e^{-i(\gamma_J - \gamma_S)\tau} e^{-i\pi S_x} e^{-i\pi I_x} \right\} \\ \times (a I_x + b S_z) \left\{ \right\}^*$$

$$= e^{-i\gamma_J 2\tau} (a I_x - b S_z) e^{+i\gamma_S 2\tau}$$

$$= -b S_z + a \left(I_x \cos(\pi J 2\tau) + I_y 2 S_z \sin(\pi J 2\tau) \right)$$

setting $2\tau = \frac{1}{2J}$, $\pi J 2\tau = \frac{\pi J}{2J} = \frac{\pi}{2}$

thus $\cos(\pi J 2\tau) = 0$, $\sin(\pi J 2\tau) = 1$

$$\rho(2\tau = \frac{1}{2J}) = -bS_z + 2aI_y S_z$$

anti-phase coherence as
 S_z has values of $+\frac{1}{2}$ and $-\frac{1}{2}$

The $(\frac{\pi}{2})_x^I$ pulse converts this into
 anti-phase S magnetization

$$\rho(t=B) = e^{-i\frac{\pi}{2}(-I_x)} (-bS_z + 2aI_y S_z) e^{i\frac{\pi}{2}(-I_x)}$$

$$= -bS_z + 2aS_z(-I_z)$$

$$= S_z(-b - 2aI_z) \quad \left\{ \begin{array}{l} \text{has 2 values} \\ -b \neq a \end{array} \right.$$

where b is equivalent to S_S
 and a is equivalent to S_I

we obtain our picture of population transfer
 by selective inversion.

Evolution of transverse magnetization in TEDOR

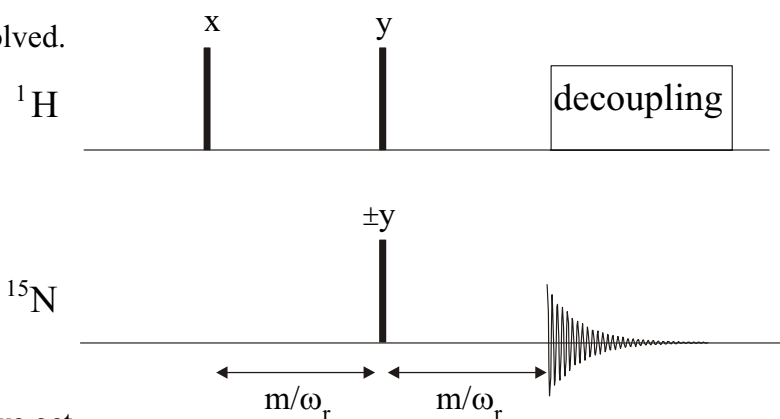
As long as we can write $\bar{\mathcal{H}}_D = Q_n I_z S_z$, product operator rules can be applied.

$$S_z \xrightarrow{Q_n I_z S_z \tau} S_z$$

$$S_x \xrightarrow{Q_n I_z S_z \tau} S_x \cos Q_n I_z \tau + S_y \sin Q_n I_z \tau = S_x \cos\left(\frac{Q_n \tau}{2}\right) + 2S_y I_z \sin\left(\frac{Q_n \tau}{2}\right)$$

$$S_y \xrightarrow{Q_n I_z S_z \tau} S_y \cos Q_n I_z \tau - S_x \sin Q_n I_z \tau = S_y \cos\left(\frac{Q_n \tau}{2}\right) - 2S_x I_z \sin\left(\frac{Q_n \tau}{2}\right)$$

The signal in a standard TEDOR arises from the following basic scheme. The initial evolution period makes anti-phase ^1H magnetization, which is refocused to generate in phase ^{15}N coherence. Both intervals are the same length of time $t = m/\omega_r = m\tau_r$, where m is the number of rotor periods involved.



Starting with H_z we get

$$H_z \xrightarrow{\left(\frac{\pi}{2}\right)_x^H} -H_y \xrightarrow{Q_n H_z N_z m\tau_r} -H_y \cos(Q_n m\tau_r / 2) + 2H_x N_z \sin(Q_n m\tau_r / 2)$$

converting to ^{15}N magnetization and rephasing gives

$$-H_y \cos(Q_n m\tau_r / 2) + 2H_x N_z \sin(Q_n m\tau_r / 2) \xrightarrow{\left(\frac{\pi}{2}\right)_y^H} -H_y \cos(Q_n m\tau_r / 2) - 2H_z N_z \sin(Q_n m\tau_r / 2)$$

$$\xrightarrow{\left(\frac{\pi}{2}\right)_y^N} -H_y \cos(Q_n m\tau_r / 2) - 2H_z N_x \sin(Q_n m\tau_r / 2)$$

$$\begin{aligned} \xrightarrow{Q_n H_z N_z m\tau_r} & -H_y \cos^2(Q_n m\tau_r / 2) + H_x \cos(Q_n m\tau_r / 2) \sin(Q_n m\tau_r / 2) \\ & - 2H_z N_x \sin(Q_n m\tau_r / 2) \cos(Q_n m\tau_r / 2) \\ & - 4H_z^2 N_y \sin^2(Q_n m\tau_r / 2) \end{aligned}$$

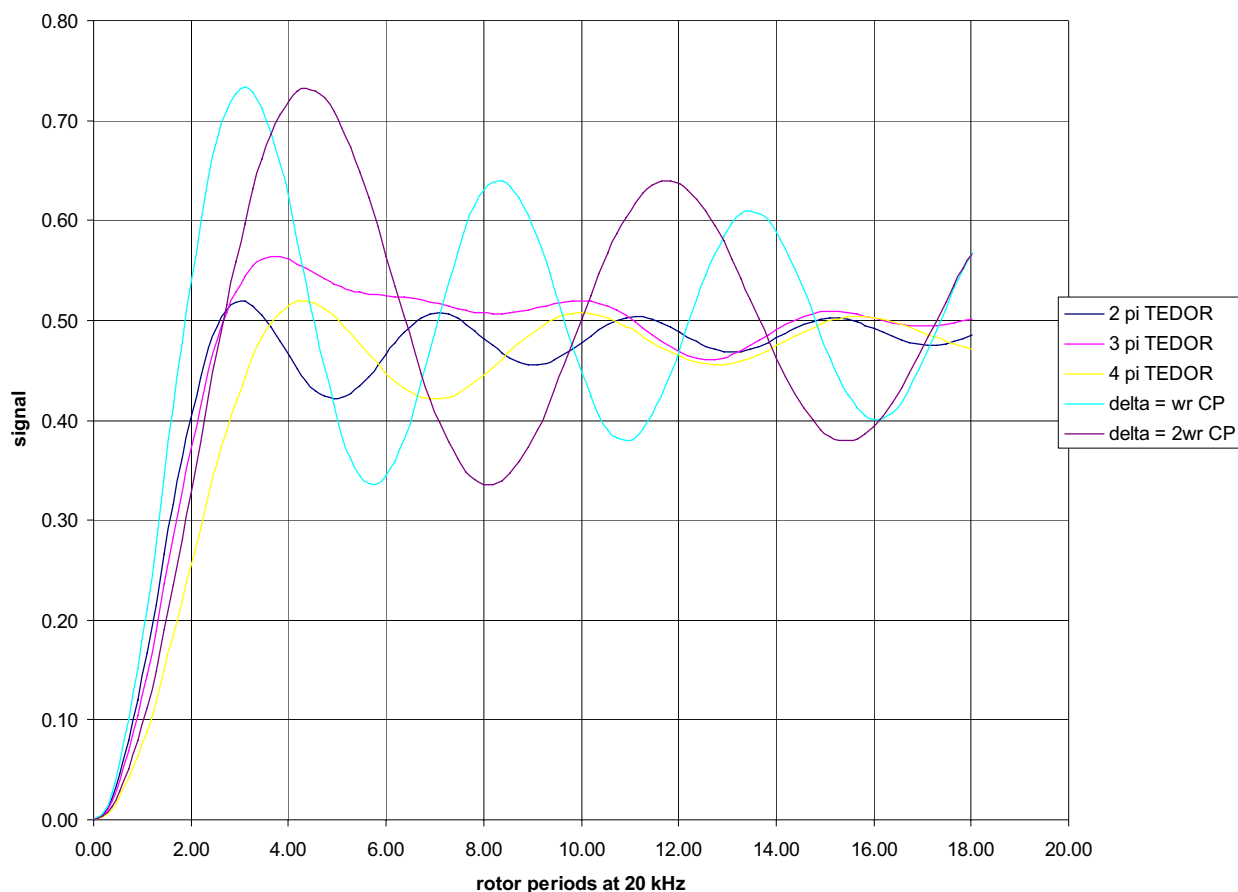
Only the last term gives observable ^{15}N transverse magnetization. The TEDOR_{1/2} signal then is

proportional to $-N_y \sin^2(Q_{1/2} m \tau_r / 2)$, where we have use the fact that $H_z^2 = \frac{1}{4}$. The TEDOR_{1/4} signal is the same except for replacing $Q_{1/2}$ by $Q_{1/4}$.

Simulating either the CP or the TEDOR signal growth curves is simplified by using a time unit that is based on the rotor cycle. Using $\nu_{IS} = D_{IS} / 2\pi$, we can write a dimensionless time axis as $m\nu_{IS} / \nu_r$. This gives us a convenient way for a given spin rate ν_r to rewrite the CP time evolution in terms of the number of rotor cycles, which is the natural time base for the TEDOR experiment.

Below we plot the signal growth for a single $^{15}\text{N}-^1\text{H}$ pair at either the $k = 1$ or 2 sideband match from a powder sum over β . A spin rate of 20 kHz and a $\nu_{IS} = D_{IS} / 2\pi = 10,990$ Hz was assumed. This corresponds to a 1.03 \AA $^{15}\text{N}-^1\text{H}$ bond length. TEDOR curves are also given for the 2 cases presented here. For the TEDOR buildup profiles the time axis corresponds to the number of rotor periods before the rephasing interval begins. Thus the total TEDOR transfer takes twice as many rotor periods as indicated on the plot.

CP and TEDOR buildup curves for NH at 20 kHz



Oxford 4.2 K

63 mm bore magnet

probe 2.0 inch O.D.

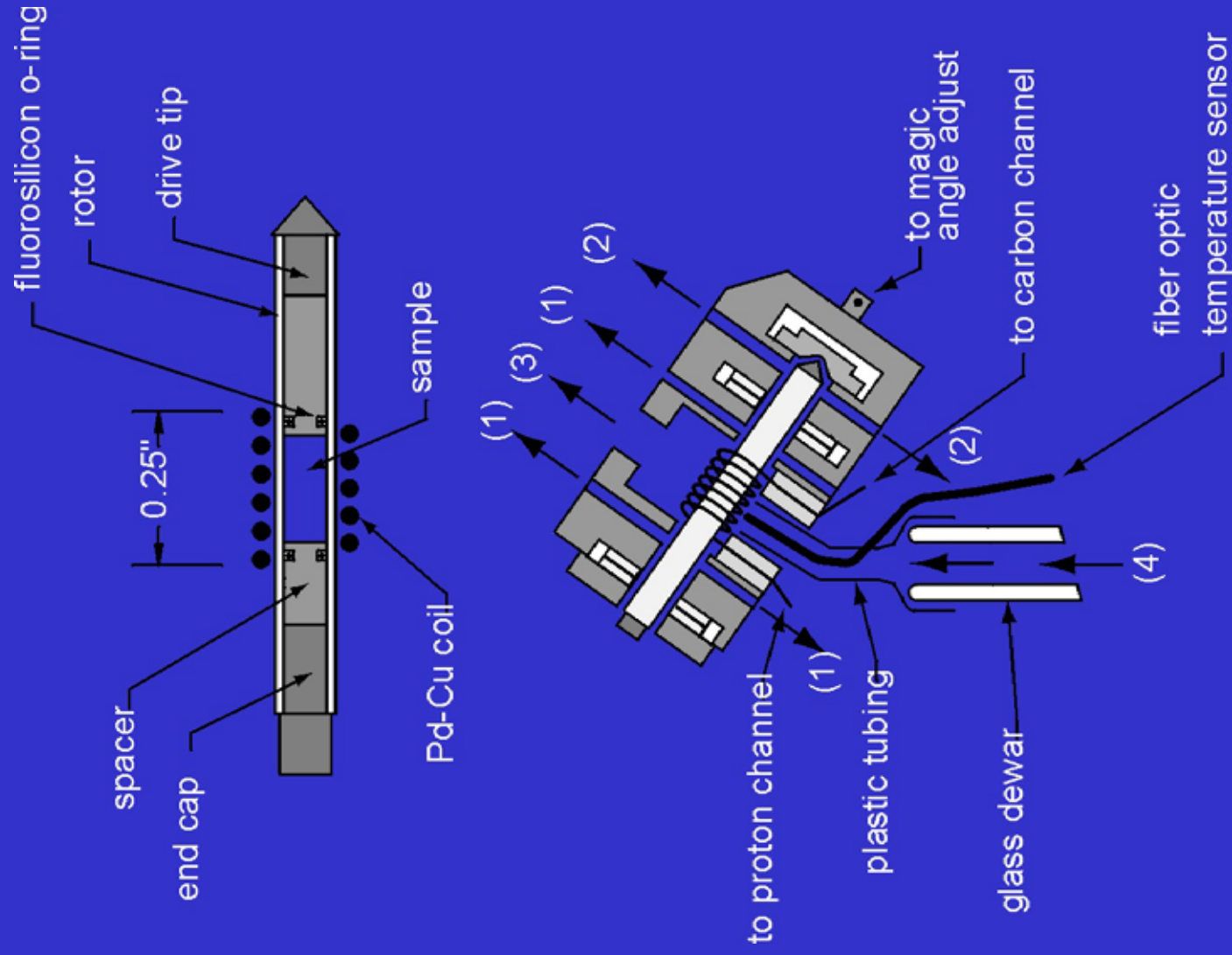


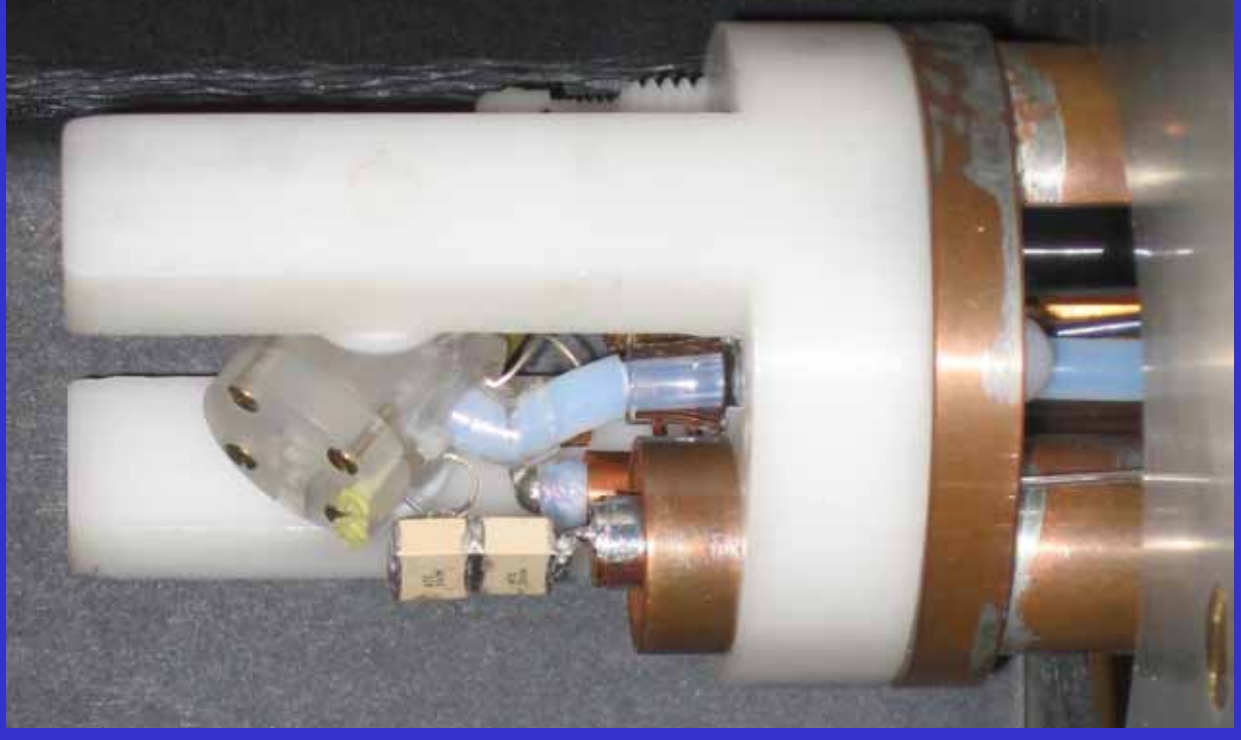
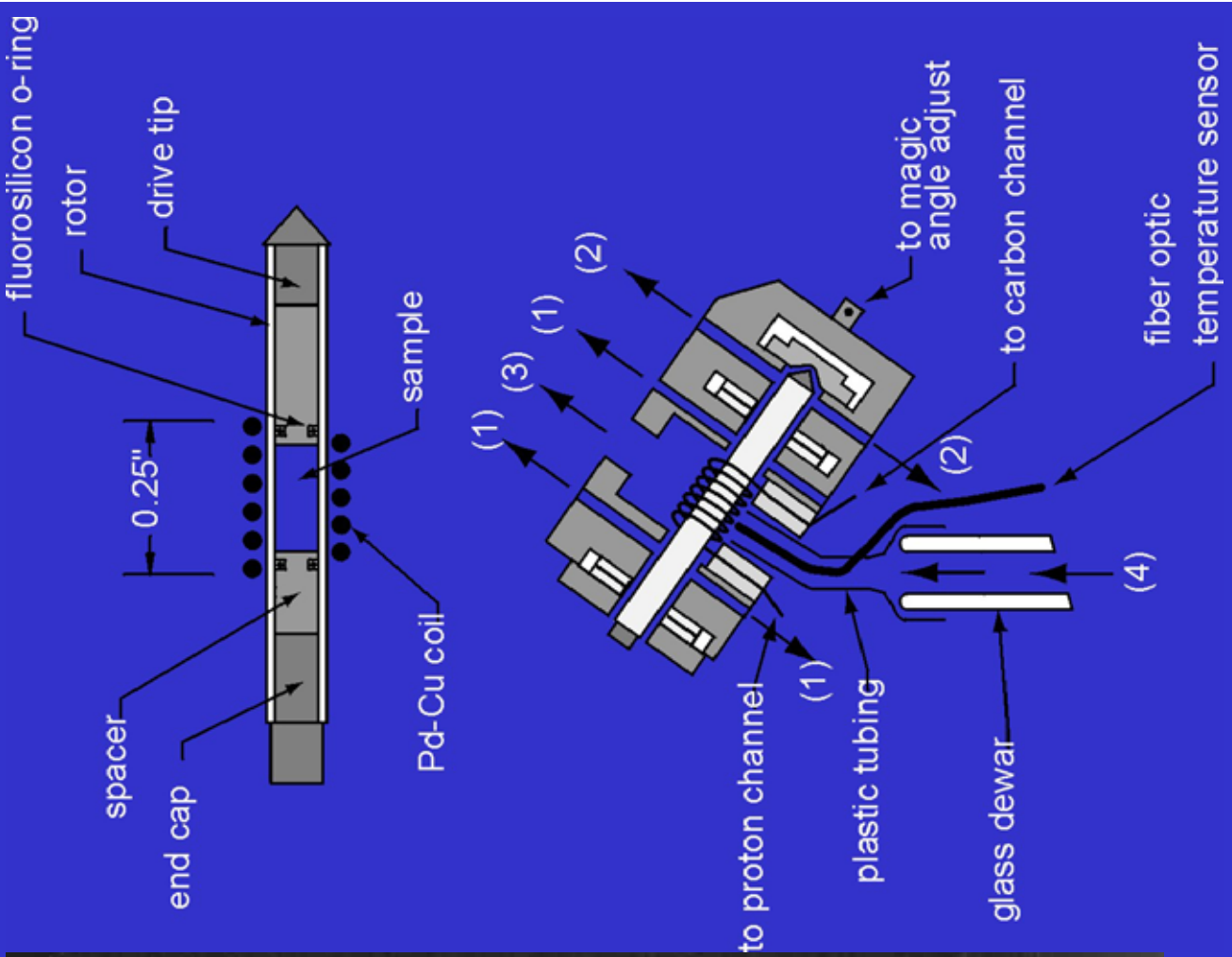
sealed rotors for VT



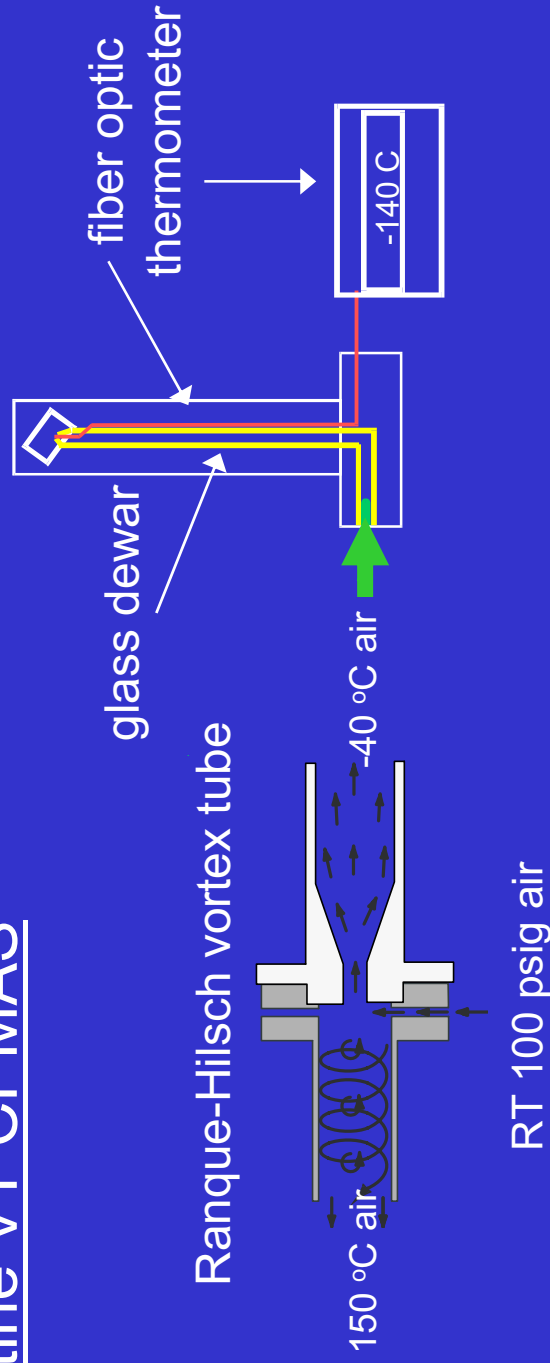
2.5 mm rotor sample
volume ~ 6.5 μ liters

1.6 mm rotor sample
volume ~ 4.5 μ liters





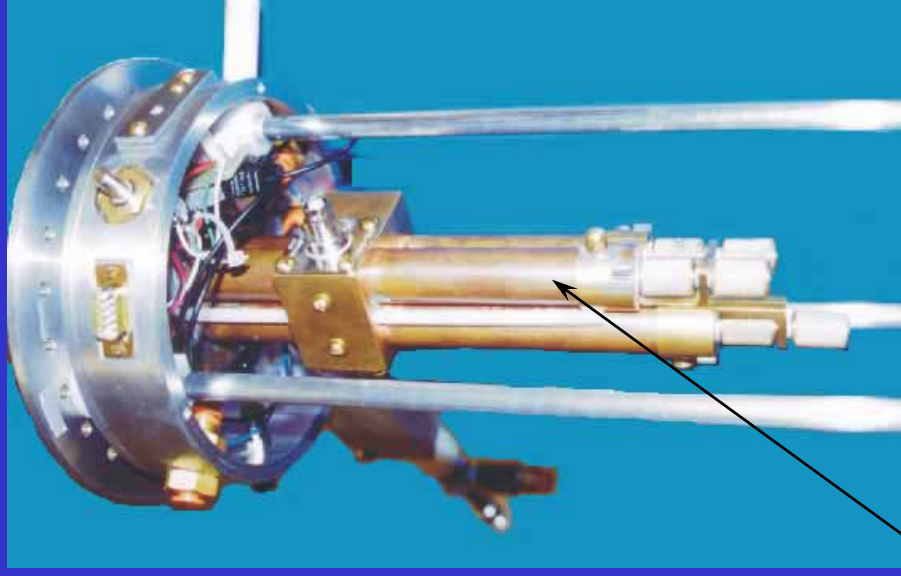
routine VT CPMAS



fiber optic thermometer

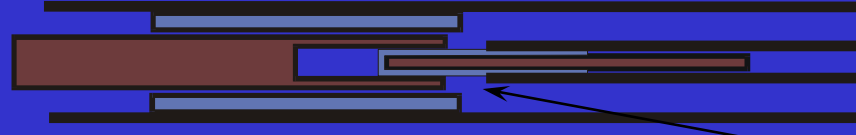
- GaAs based
- measures band edge
- ~ -16 K offset @ 18T
- NeOptix

an 800 MHz $^1\text{H}/^{13}\text{C}/^{15}\text{N}$ tuning tube probe



tuning tubes

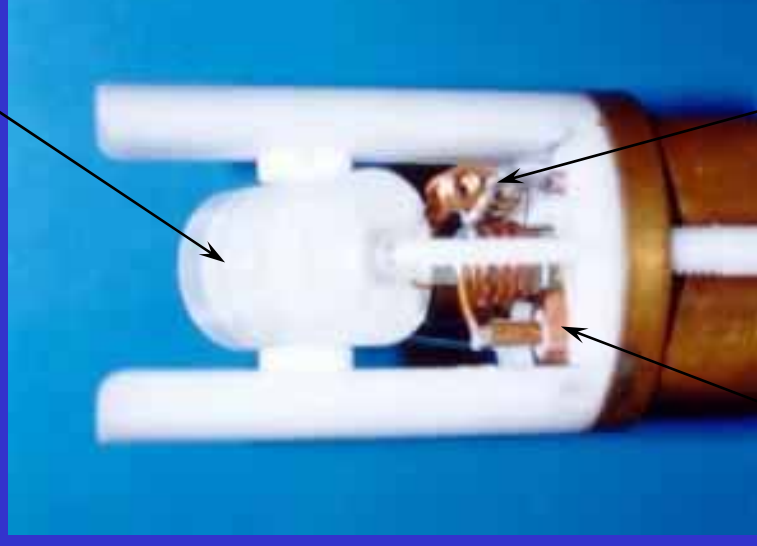
teflon tuning slug



50 W coax input

match capacitor

2.5 mm Kel-F Pencil stator



balancing trap

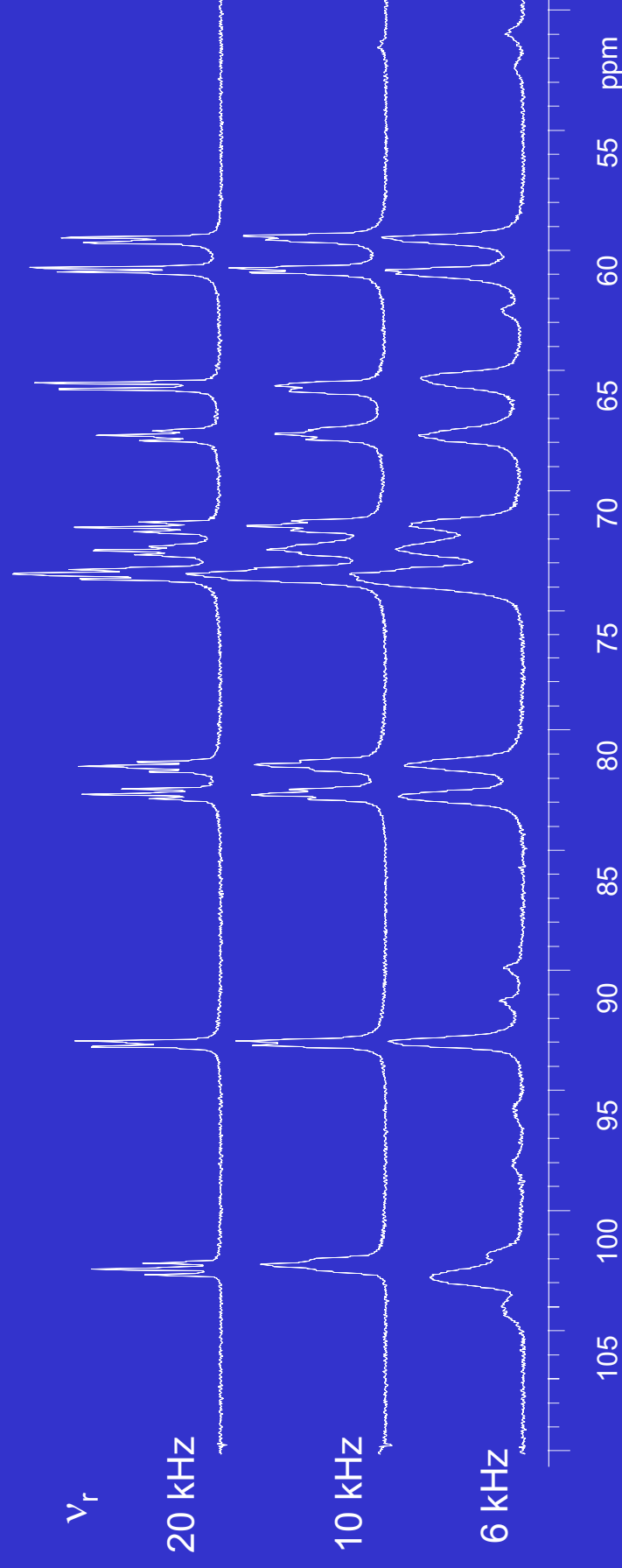
^{13}C trap

Table I
Triple Resonance Performance Data and Modeling Results

nucleus	Frequency (MHz)	Power (W)	90° pulse (μsec)	B_1 / i_{input} (mT · A ⁻¹)	$\sqrt{\frac{\eta_i}{\eta_{13C}}}$	$\left(\frac{i_{\text{coil}}}{i_{\text{input}}}\right)_{\text{calculated}}$	$(B_1 / i_{\text{input}})_{\text{calculated}}$ (mT · A ⁻¹) ^a	$\left(\frac{i_{\text{coil}}}{i_{\text{input}}}\right)_{i_{\text{ideal}}}$	$\Xi = \frac{i_{\text{triple probe}}}{i_{i_{\text{ideal probe}}}}$
¹ H	800.0	120	1.9	1.41	0.61	3.02	1.35	6.45	0.47
¹³ C	201.1	100	3.6	3.24	1.00	6.72	3.01	11.51	0.58
¹⁵ N	80.1	640	2.9	3.95	0.97	10.07	4.52	16.00	0.63

a) assuming $n' \approx (\text{turns} - 1) / (\text{coil length} - \text{wire diameter}) \approx 875 \text{ turns} \cdot \text{m}^{-1}$ as an approximation for a 0.25 inch long 6 turn finite length coil constructed from 0.025 inch diameter wire.

relatively fast MAS required for high resolution with uniform ^{13}C enrichment



200 MHz CPMAS spectra of $u\text{-}^{13}\text{C}$ sucrose

requires attention to VT and CP transfer stability

CP signal buildup theory

$$\langle S_x(\tau) \rangle = \frac{|b_k|^2}{|b_k|^2 + (\Delta - k\omega_r)^2} \sin^2 \left\{ \frac{\tau}{2} \sqrt{|b_k|^2 + (\Delta - k\omega_r)^2} \right\}$$

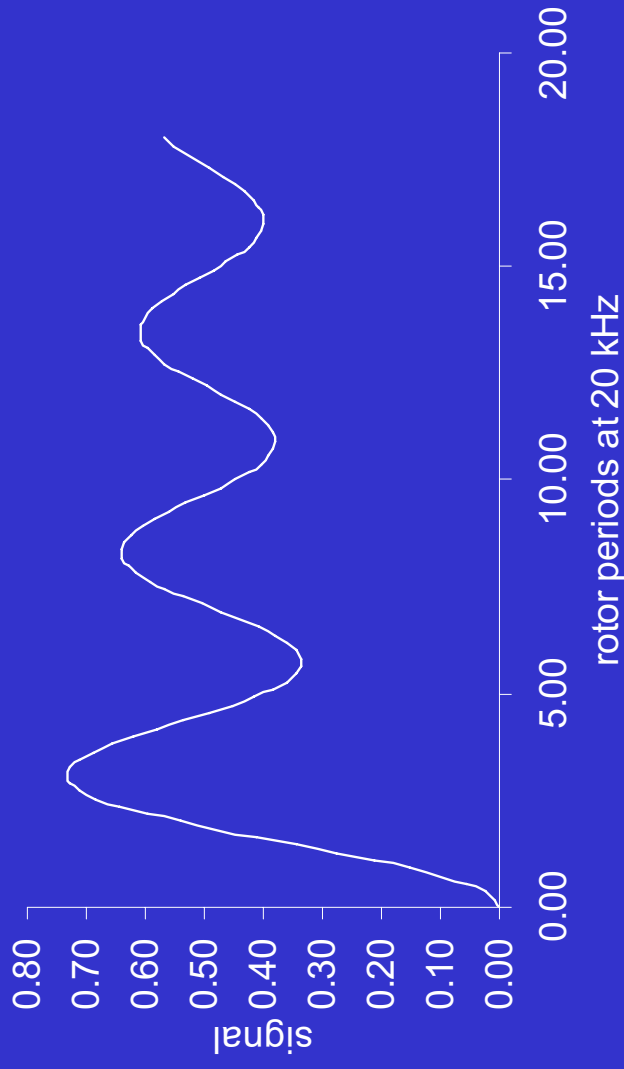
$$b_{\pm 1} = -b_{1s} \sqrt{2} \sin(2\beta) e^{\pm i\gamma}$$

$$b_{\pm 2} = -b_{1s} \sin^2 \beta e^{\pm 2i\gamma}$$

$$\Delta = \omega_{11} - \omega_{1s}$$

$$b_{1s} = \frac{\mu_o \gamma_1 \gamma_s \hbar}{4\pi 4r^3}$$

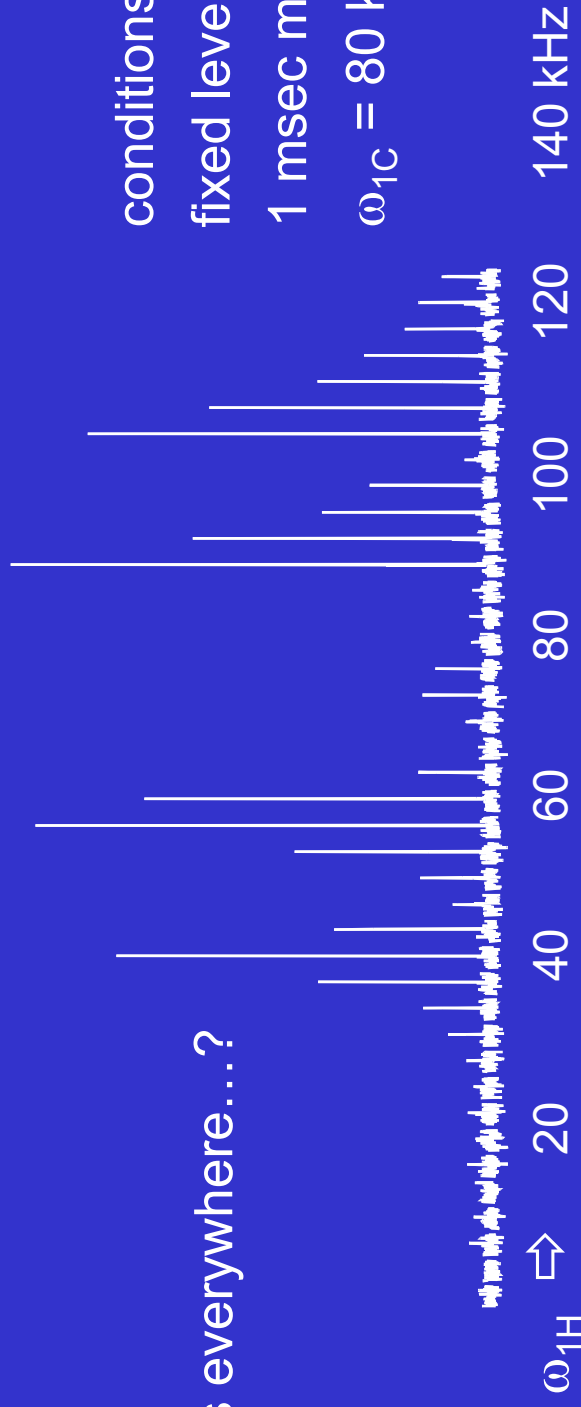
CP buildup curve for NH at 20 kHz



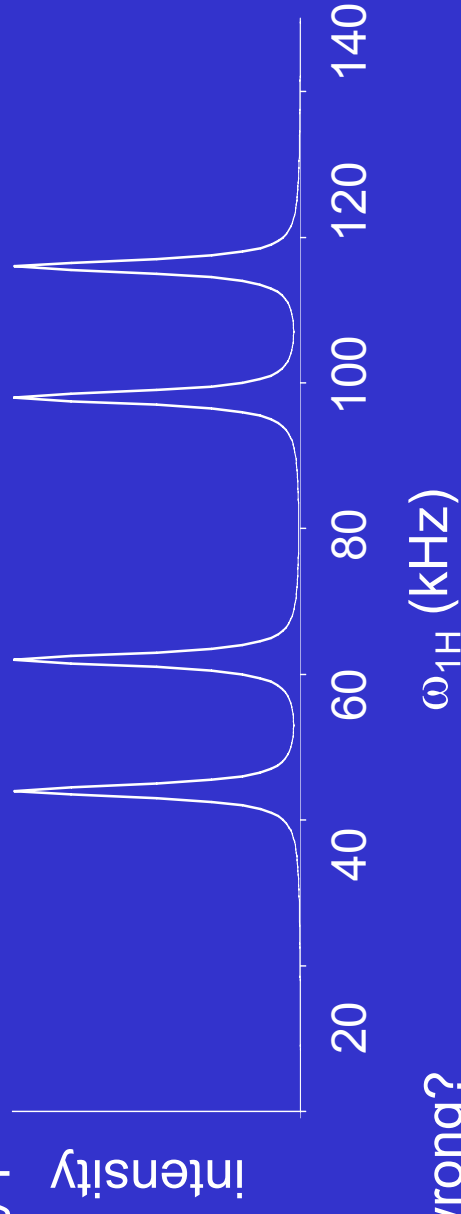
an adamantane CP matching curve at $\nu_f = 19$ kHz

matches everywhere....?

conditions:
fixed level CP
1 msec match
 $\omega_{1C} = 80$ kHz

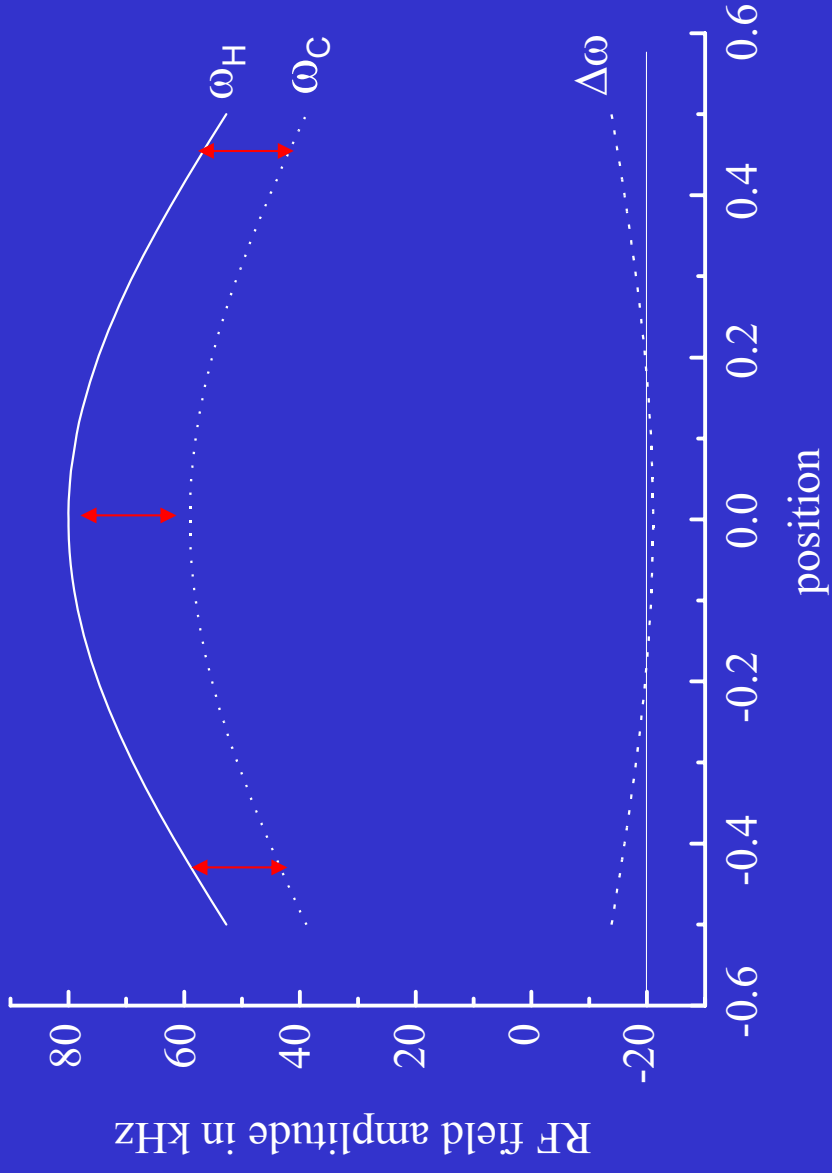


but theory predicts....



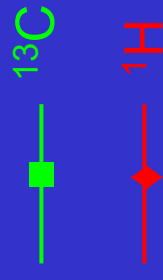
what's wrong?

CP matching in an inhomogeneous RF field

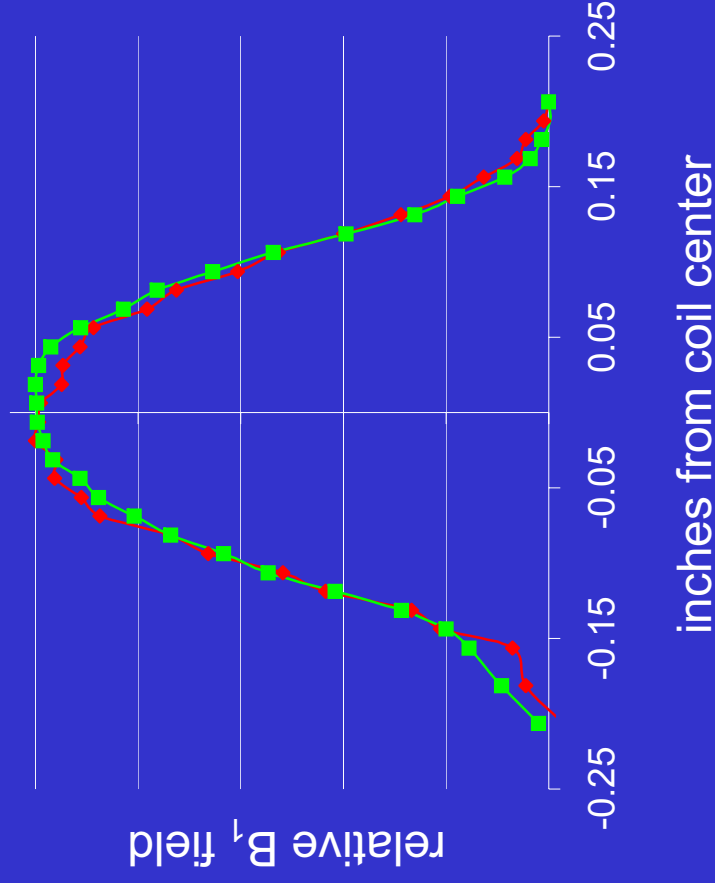


cannot set $\omega_H = \omega_C + \omega_R$ everywhere at once

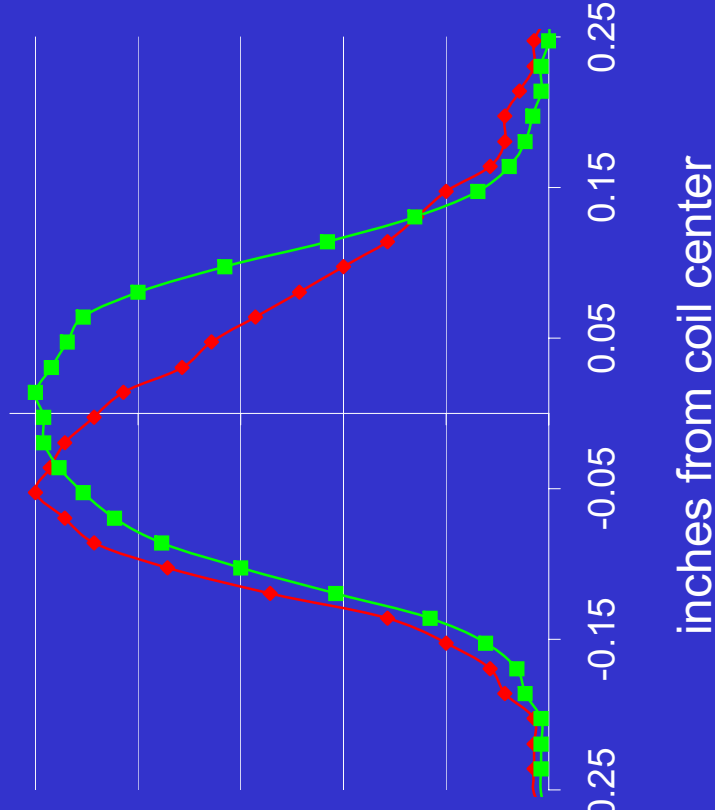
B₁ inhomogeneity and wavelength



expected B₁ field profiles



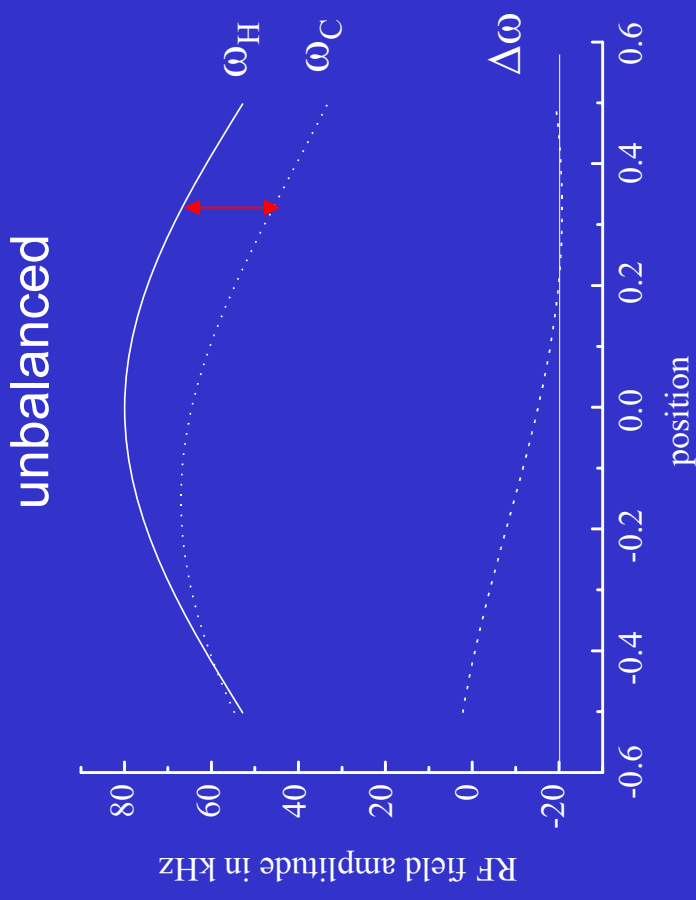
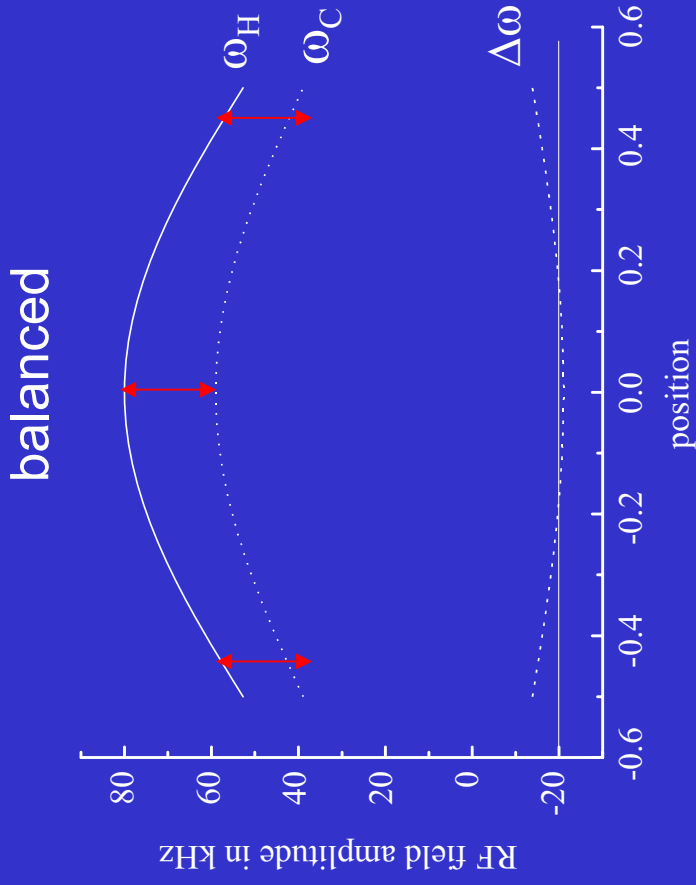
measured B₁ field profiles



relative B₁ field measured by:

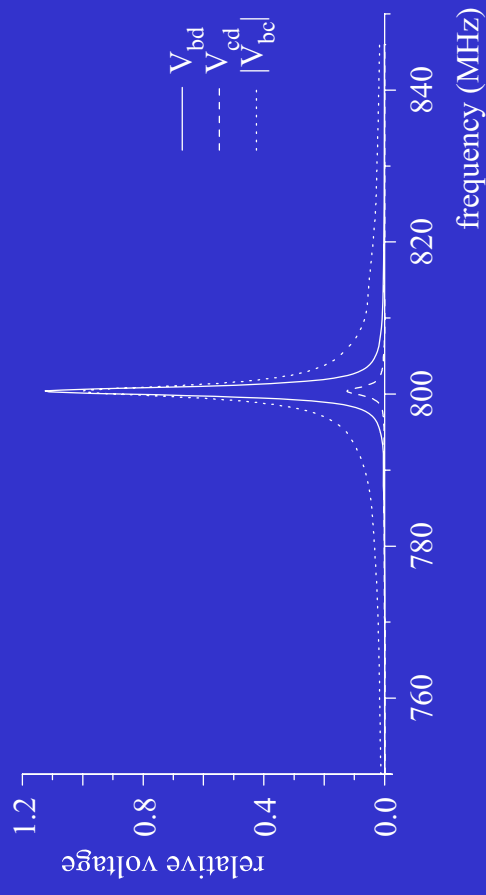
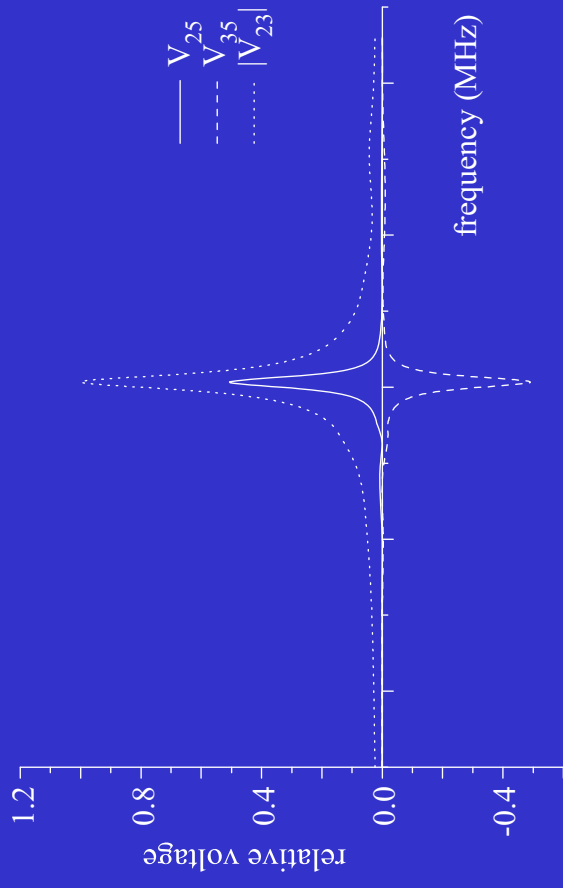
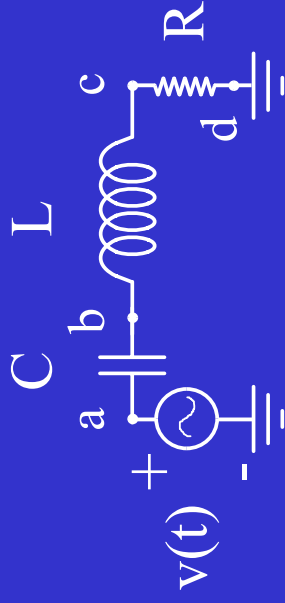
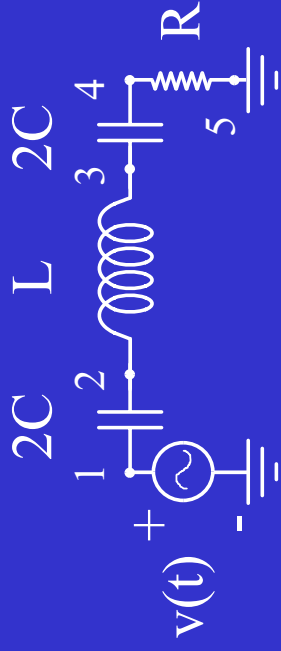
- * nutation on thin sample vs. position
- * nutation image in a static field gradient
- * shift of tuning versus position of small piece of Cu

CP matching in an inhomogeneous RF field

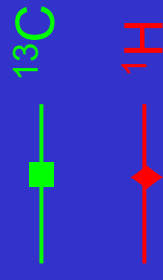


cannot set $\omega_H = \omega_C + \omega_R$ everywhere at once

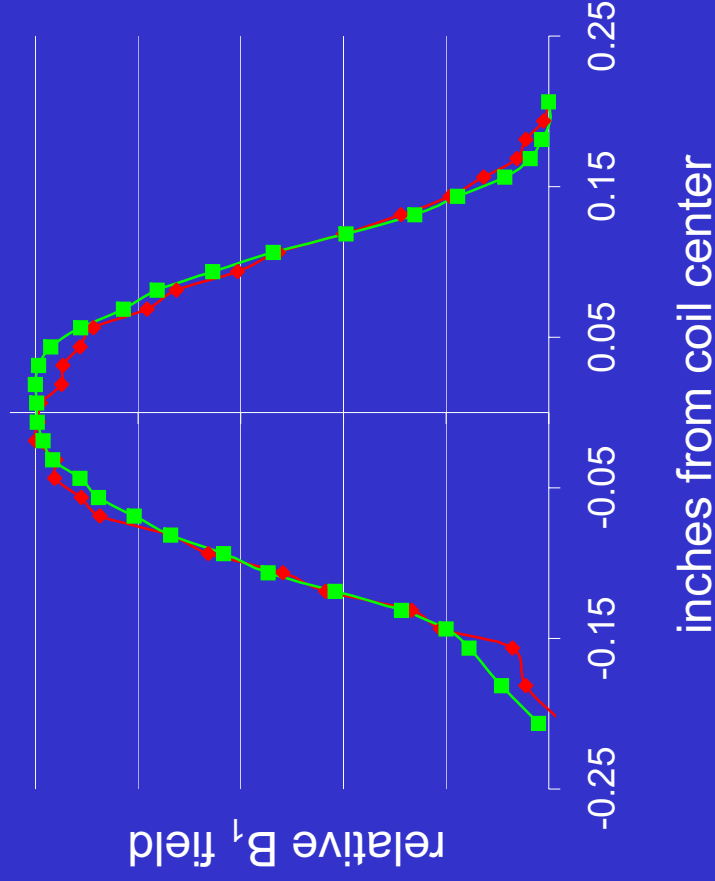
balanced vs. unbalanced probes



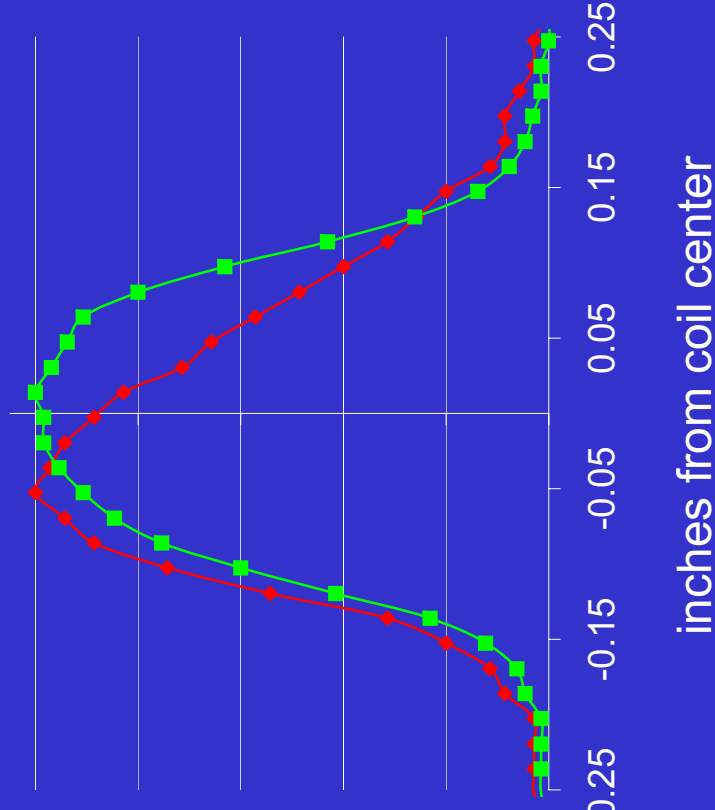
B₁ inhomogeneity and wavelength



balanced B₁ field profiles



unbalanced B₁ field profiles



relative B₁ field measured by:

* nutation on thin sample vs. position

* nutation image in a static field gradient

* shift of tuning versus position of small piece of Cu

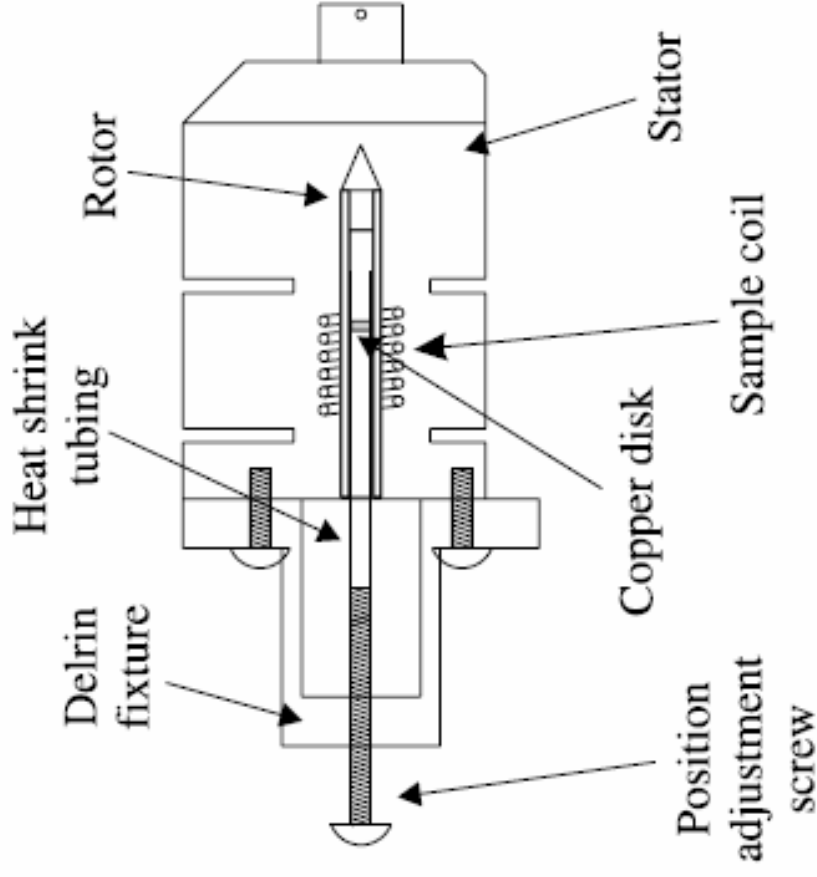
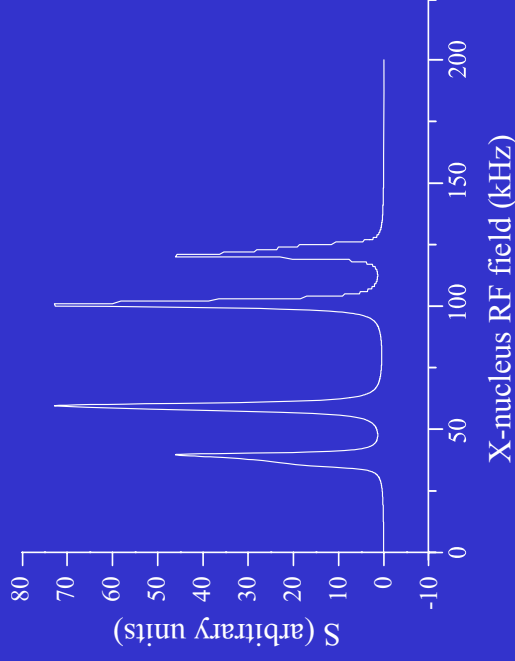


Fig. 8. Apparatus for electronically measuring the magnetic field profile inside the rotor, shown in cross section as affixed to the Chemagnetics 2.5 mm MAS stator. As the copper disk is incrementally positioned along the axis of the rotor by advancing the screw, the tuning frequency is monitored on the channel of interest. Frequency deflections are proportional to the square of the magnetic field at each point in the coil.

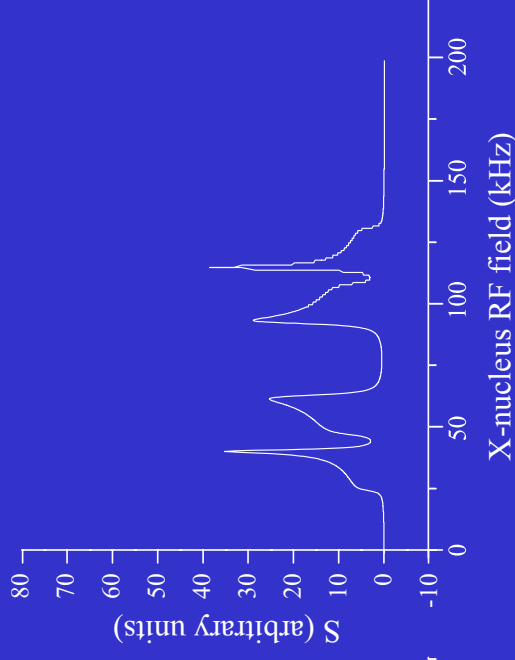
matching envelope as a function of RF homogeneity and field offset

offset = 0.0

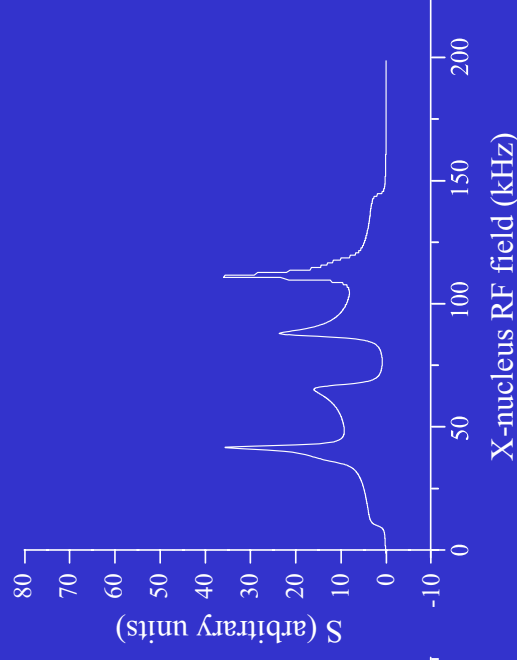
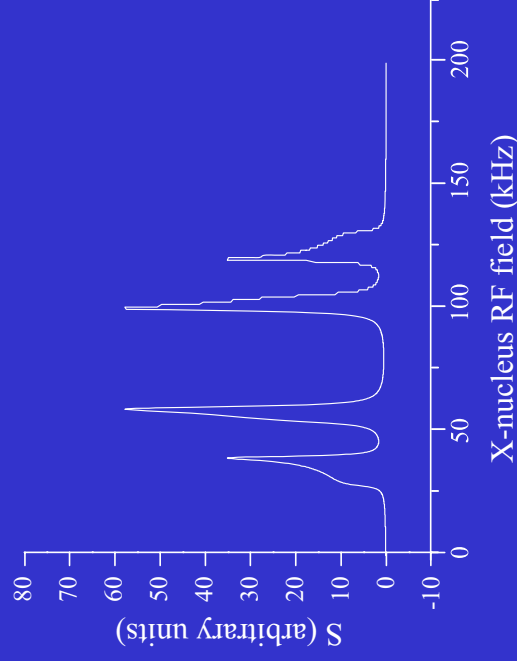


$810^\circ/90^\circ = 90\%$

offset = 0.2

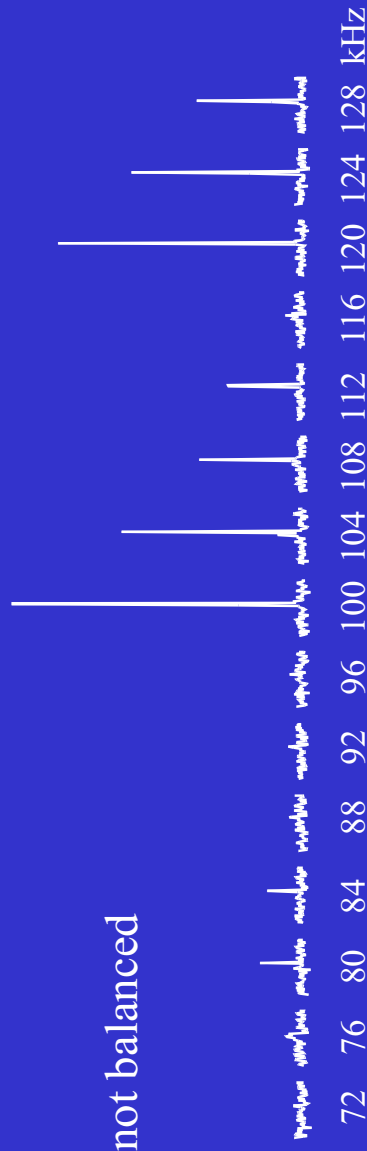


$810^\circ/90^\circ = 65\%$

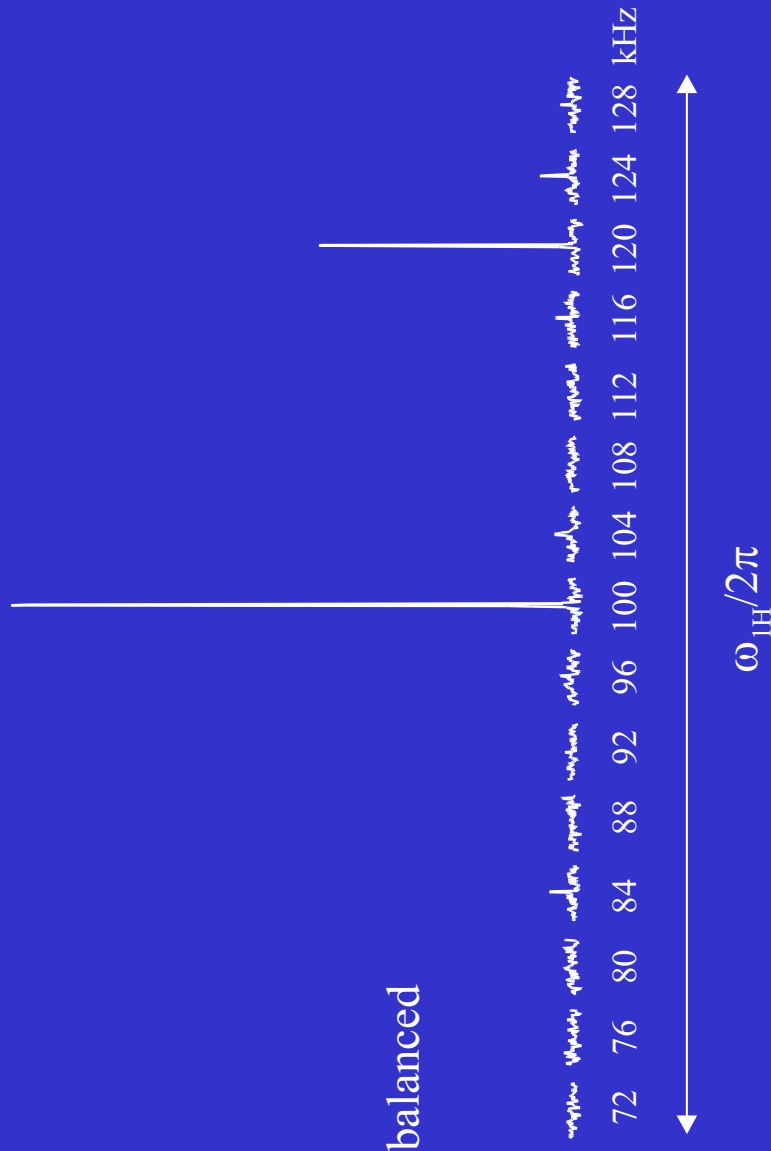


adamantane matching arrays at $\omega_r = 20$ kHz

not balanced

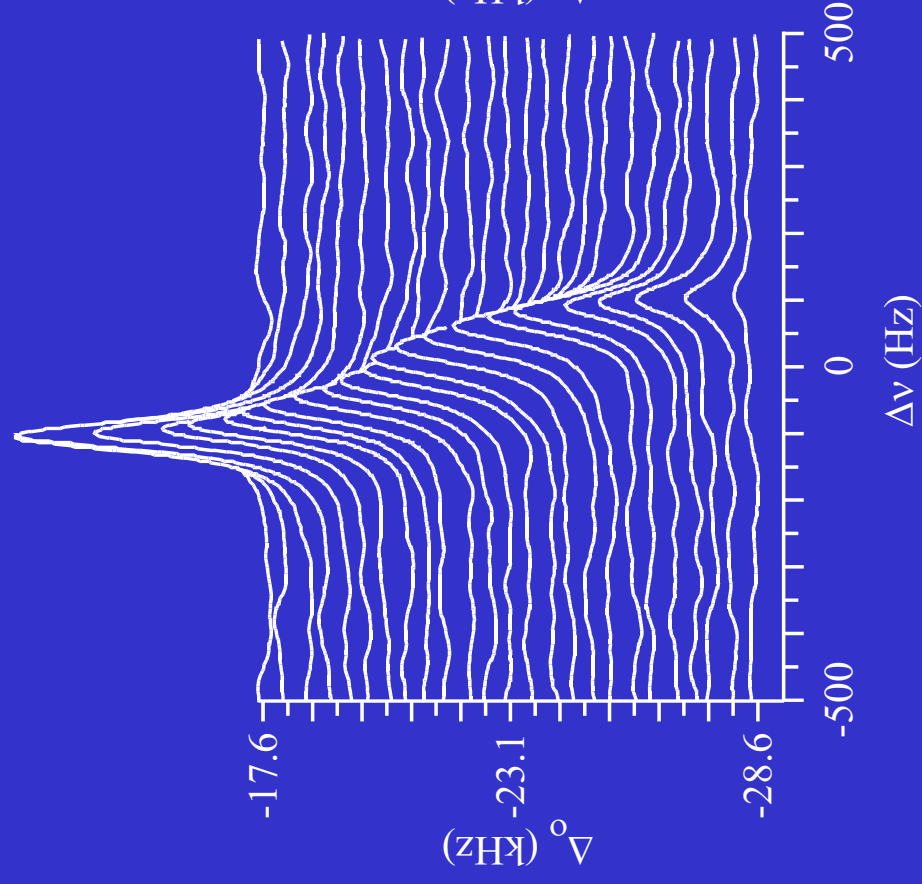


balanced

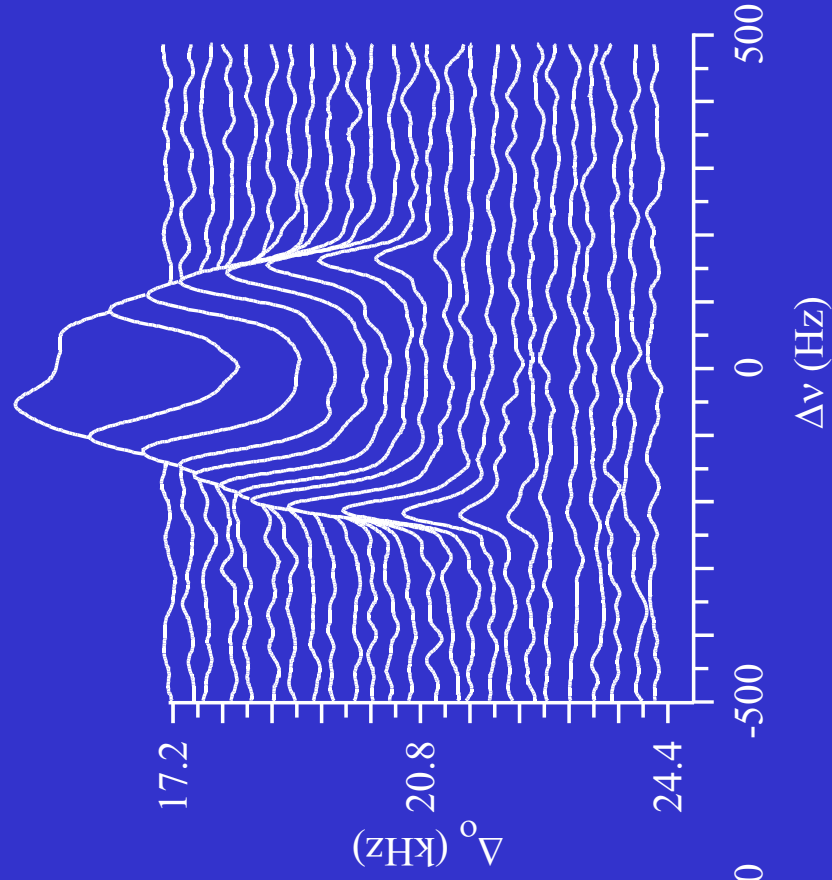


CP matching images for adamantane in a static field gradient

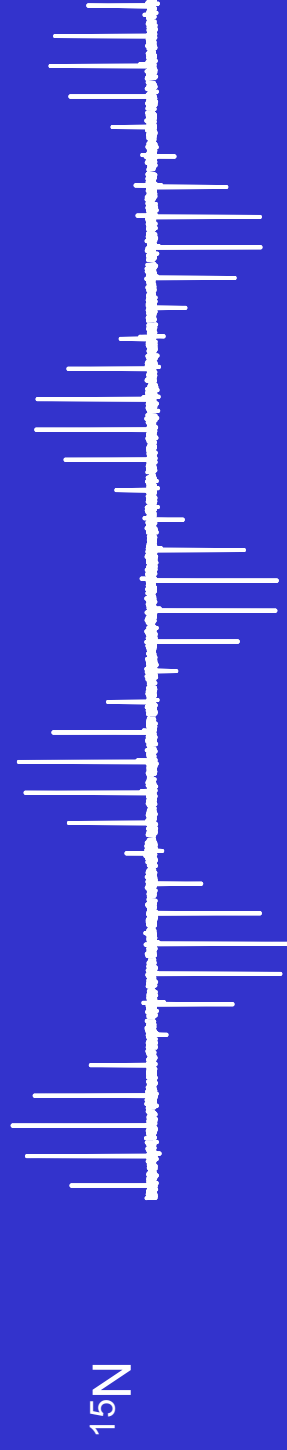
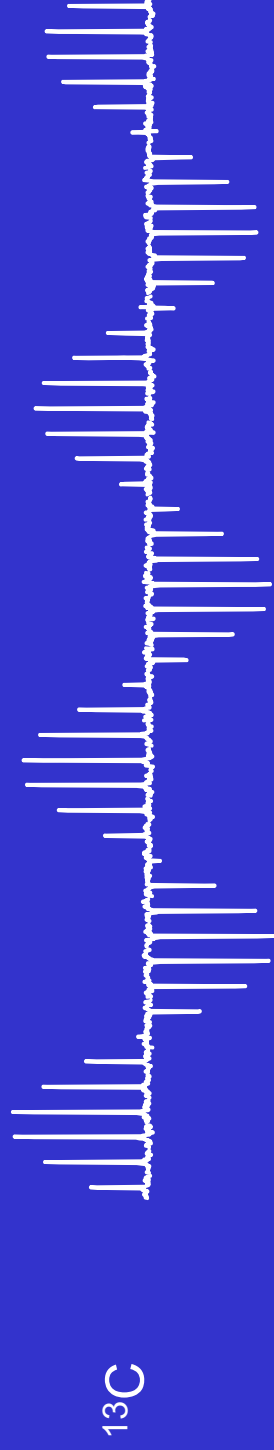
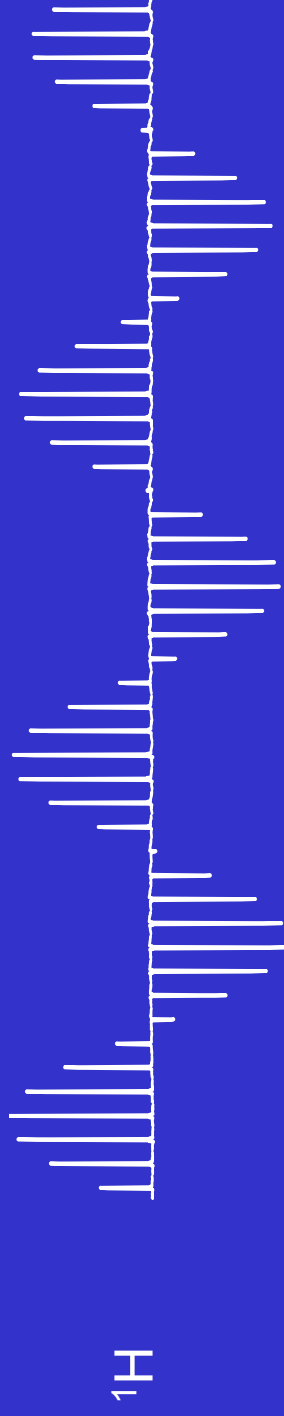
unbalanced



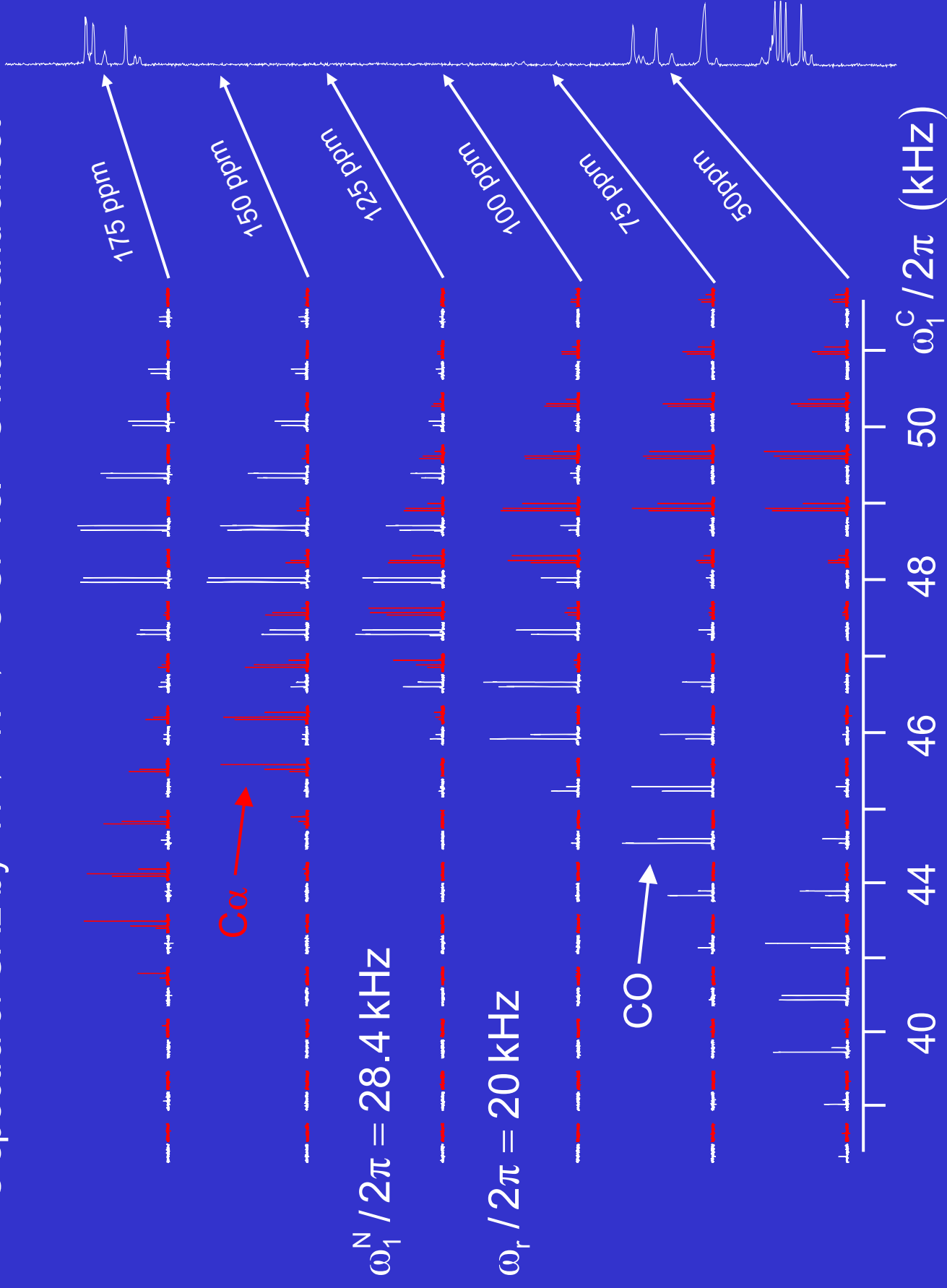
balanced



RF homogeneity by nutation arrays



^{13}C spectra of GAL by $^1\text{H} \rightarrow ^{15}\text{N} \rightarrow ^{13}\text{C}$ CP vs. ^{13}C match and offset



Basic AC circuit theory for resonant RLC circuits

In a simple RLC circuit subjected to a sinusoidal voltage, the instantaneous voltages $\bar{v}(t)$ across components follow the following equations. For the resistor

$$\bar{v}(t) = R\bar{i}(t)$$

the capacitor

$$\bar{v}(t) = q(t)/C \text{ or } \frac{d\bar{v}(t)}{dt} = \frac{1}{C}\bar{i}(t)$$

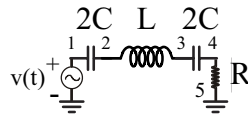
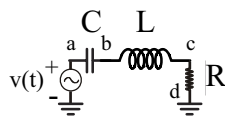
and for the inductor

$$\bar{v}(t) = L\frac{d\bar{i}(t)}{dt}$$

As long as the frequency is not so high that wavelength effects are not an issue, the instantaneous current $\bar{i}(t)$ can be taken as the same at all points. As steady state the current-voltage relation across any single component is fixed by the complex impedance through

$$\bar{v}_{kl}(t) = Z_{kl}\bar{i}(t)$$

For the resistor $Z = R$, for an inductor $Z = j\omega L$, and for a capacitor $Z = 1/j\omega C$, where we have used $j = \sqrt{-1}$ to avoid confusion with $\bar{i}(t)$. Now consider the two simple circuits below.



The voltage source provides a voltage

$$v(t) = v_{ad}(t) = v_o e^{j\omega t}$$

If the frequency is chosen as the resonant frequency where

$$LC = 1/\omega^2$$

the net series impedance

$$Z_{ad} = Z_c + Z_L + Z_R = j\omega L + 1/j\omega C + R$$

since

$$j\omega L + 1/j\omega C = j(\omega L - 1/\omega C) = 0$$

$$Z_{ad} = R$$

And

$$i_{ad}(t) = i_{cd}(t) = i(t) = v(t)/R.$$

The voltage across the capacitor C is given by

$$v_{ab}(t) = Z_{ab} i_{ab}(t) = -(j/\omega C) i(t)$$

Substituting for the current

$$v_{ab}(t) = -(j/\omega C) v(t)/R = (1/\omega CR) v(t) e^{-j\pi/2}$$

where the last step follows from DeMivre's theorem. If the resistance R is taken to be the equivalent series resistance for the inductor L, we can substitute using the definition of the quality factor

$$Q = \omega L/R$$

Using the resonance condition $\omega L = 1/\omega C$, we arrive at the result that the voltage across the capacitor at resonance is

$$v_{ab}(t) = Q v(t) e^{-j\pi/2}$$

This is Q times the applied voltage and out of phase by $-\pi/2$. It likewise follows that the voltage across the inductor

$$v_{bc}(t) = Z_{bc} i(t) = j\omega L v(t)/R$$

or $jQ v(t)$, which is equivalent to $Q v(t) e^{j\pi/2}$. Thus

$$v_{bc}(t) = -v_{ab}(t) \text{ as } e^{j\pi/2} = j = -(e^{-j\pi/2}) = -(-j)$$

and

$$v_{ac}(t) = v_{ab}(t) - v_{bc}(t) = 0$$

as expected.

In the second circuit the same inductance and resistance are used, but the capacitance is split across the inductor. This has the same resonance frequency as

$$Z_{14} = -j/2\omega C + j\omega L - j/2\omega C = -j/\omega C + j\omega L = Z_{ac}.$$

Therefore the current is the same for the same $v(t)$. Thus

$$v_{12}(t) = -(j/2\omega C) v(t)/R = (1/2\omega CR) v(t) e^{-j\pi/2} = (Q/2) v(t) e^{-j\pi/2}$$

The voltage across the inductor is still the same

$$v_{23} = Q v(t) e^{j\pi/2}$$

and the voltage across the second capacitor is

$$v_{34} = (Q/2) v(t) e^{-j\pi/2}$$

As before, since the circuit is resonant, the voltage

$$v_{14} = (Q/2) v(t) e^{-j\pi/2} + Q v(t) e^{j\pi/2} + (Q/2) v(t) e^{-j\pi/2} = 0.$$

The main difference between the circuits arises when the voltages at the various points are considered relative to the ground plane. In the first circuit the voltage v_{bd} at the junction of the capacitor and inductor relative to ground is $v_{bc} + v_{cd}$. As long as R is small, i.e. Q high,

$$v_{bd} \sim v_{bc} = Q v(t) e^{j\pi/2}$$

In the second circuit the voltage relative to ground at the first junction is

$$v_{23} + v_{34} = Q v(t) e^{j\pi/2} + (Q/2) v(t) e^{-j\pi/2} = (Q/2) v(t) e^{+j\pi/2}$$

At the second junction this is just

$$v_{34} = (Q/2) v(t) e^{-j\pi/2}$$

The voltage rise with respect to ground then is half the amplitude of that in the single ended circuit. Both ends of the inductor experience the same voltage swing with respect to the ground plane, but these are out of phase by π at any point in time.

The advantage of the double ended or “balanced” circuit is that the inductor is more symmetrically driven. Equivalent charge flows from one capacitor to the other through the inductor, and this should be true even if the inductor is a less than ideal element. Any perturbations of the environment on the inductor by coupling through the electric fields will also be symmetric, as the voltages present will be symmetrical at both ends of the inductor when measured relative to ground.